The oldest articulated ranid from Europe: a Pelophylax specimen from the lowest Oligocene of Chartres-de-Bretagne (N.W. France)

Alfred Lemierre, Damien Gendry, Marie-Margaux Poirier, Valentin Gillet, Romain Vullo

ARTICLE

The oldest articulated ranid from Europe: A *Pelophylax* specimen from the earliest Oligocene of Chartres-de -Bretagne (NW France)

ALFRED LEMIERRE,*[,1] DAMIEN GENDRY,[2] MARIE-MARGAUX POIRIER,[2] VALENTIN GILLET,[2] and ROMAIN VULLO[2]

[1]Centre de Recherche en Paléontologie (CR2P) Paris, UMR 7207 CNRS-Muséum National d'Histoire Naturelle-Sorbonne Université, CP38, 8 rue Buffon, 75005 Paris, France, alfred.lemierre@outlook.com;

[2]Université Rennes, Géosciences, UMR CNRS 6118, Campus de Beaulieu, 263 avenue du Général Leclerc, 35042 Rennes, France, mariemargaux.poirier@orange.fr, valentin.gillet.37@gmail.com, romain.vullo@univ-rennes.fr, damien.gendry@univ-rennes.fr

* Corresponding author

ABSTRACT—Ranids represent an important part of the extant anuran diversity of Europe. One of the best-known genera is *Pelophylax* (green-water frog). This genus is considered to have arrived in Europe during the Eocene/Oligocene transition, with numerous occurrences of the genus throughout European Oligocene sites. Unfortunately, most of the specimens are isolated bones, hampering our understanding of the diversity and evolution of the genus during this time. We here present the description of an incomplete but articulated anuran skeleton from the earliest Oligocene of Chartres-de-Bretagne (Western France). This specimen, missing its head, preserves almost all postcranial bones articulated and skin impressions. The osteological description allows to assign this specimen to *Pelophylax* kl. *esculentus,* making it one of the oldest known occurrences of the genus. We also suggest that specimens assigned to the late Oligocene "*Rana*" *aquensis* should be referred to the genus *Pelophylax*. The presence of a *Pelophylax* in Western Europe during the early Oligocene indicates that the genus had already spread throughout Europe, no later than 5 Ma after its emergence in the eastern part of the continent. It suggests that *Pelophylax* benefitted from the extinction of ranoids during the "Grande Coupure."

SUPPLEMENTAL DATA—Supplemental materials are available for this article for free at www.tandfonline.com/UJVP

Submitted October 19, 2022; revisions received March 09, 2023; accepted Month DD, YYYY.
Handling Editor: Hans-Dieter Sues.

INTRODUCTION

Anurans have been recovered from numerous Cenozoic sites in Europe, documenting a rich and diverse history of the clade during this period. In peculiar, the Quercy Phosphorites (mostly Eocene/Oligocene deposits; Pélissié et al., 2021) have yielded hundreds of anurans bones, representing most extant anuran clades present in Europe (Rage, 2016). The Phosphorites also document the turnover within neobatrachians anurans during the "Grande Coupure," with the establishment of "true" ranid taxa during the Oligocene (Rage, 2016; Vasilyan, 2018). Among them, the genus *Pelophylax* (green-water frogs) is thought to have appeared and diversified during the early-middle Oligocene (Chan & Brown, 2017). Unfortunately, the genus is represented only by isolated bones from a single site during the early Oligocene (Sanchíz et al., 1993). Two taxa from the late Oligocene/Early Miocene, "*Rana*" *aquensis* Coquand, 1845 (southern France) and "*Rana*" *meriani* Meyer, 1852 (southern Germany), known by several complete specimens, have been informally assigned to the genus, but several uncertainties remain regarding their attribution (Sanchíz, 1998). Thus, the evolution of the geographical range of *Pelophylax* is almost unknown during a crucial phase of its spread across Western Europe, as the genus is present in most of Western Europe during the Miocene (Roček, 2013). Discovery and identification of specimens of *Pelophylax* from this region would help our understanding of the dispersal and evolutionary history of the genus during the Oligocene.

Our study is focused on the description and identification of a specimen from this geographical area (Fig. 1A, B). The specimen was discovered on July 7, 1922, by the geologist Yves Milon in the Grands-Fours quarry near the city of Rennes (Brittany, western France, Fig. 1C, D). Two days later, the specimen was presented at a session of the Société Géologique et Minéralogique de Bretagne (Dangeard & Milon, 1922). Unfortunately, Milon never described the specimen, and it was considered lost for several decades. One of us (D. Gendry) recently

rediscovered this specimen, along with Milon's identification (an anuran) in the collection of the geological museum of the University of Rennes 1. We took this opportunity to describe the osteology of the fossil and propose a taxonomic attribution. We also discuss its implication for the Oligocene occurrence of ranid taxa in Europe.

GEOLOGICAL CONTEXT

Chartres-de-Bretagne is an ancient complex of quarries located 5 km south of the city of Rennes, within the Cenozoic Basin of Rennes (Fig. 1A). The quarry produced limestone, with numerous open pits present (Vasseur, 1881; Trautmann et al., 2000; Lebrun et al., 2017). The sites are unfortunately backfilled today, and no further investigations are possible.

The Oligocene beds of Chartres-de-Bretagne are thick (380 m thick) and have been well-known since the end of the nineteenth century (Vasseur, 1881; Lebesconte, 1879; Allix, 1922; Dangeard & Milon, 1926; Lebrun et al., 2017). The Lower Sapropels Formation is the most basal formation. It forms the majority of the Oligocene deposits (around 280 m) and represents a major regression during the early Rupelian. This bed is overlain by the *Natica crassatina* marls and "*Archiacina*" limestone formations (52 m thick). These two formations were deposited during a transgressive event that lasted throughout the early Rupelian (Fig. 1B). The uppermost Oligocene formation within the region is the Upper Sapropels Formation (Rupelian; around 6.5 m thick). Within this formation, the foraminiferans *Arenagula kerfornei* and *Archiacina armorica* (*Peneroplis armorica* in Bauer et al., 2016) have been recovered (Bauer et al., 2016; Lebrun et al., 2017). In a previous study (Bauer et al., 2016), the foraminiferan *Archiacina globula* was also mentioned. However, it is a subjective junior synomyn of *Arenagula kerfornei* (World Register of Marine Species: https://www.marinespecies.org). Both *Arenagula kerfornei* and *Archiacina armorica* are early Rupelian markers for the SBZ 21 biozone (Cahuzac & Poignant, 1997; Bauer et al., 2016). Notably, they are not present in the

following SBZ 22 biozone (*Arenagula* is only present in the SBZ 22A of the Aquitaine Basin; Cahuzac & Poignant, 1997), to which a recent study (Bauer et al., 2016) attributed the Upper Sapropels Formation (at least part of it). Thus, we do not agree with this attribution, and consider the entire Upper Sapropels Formation early Rupelian in age (SBZ 21 biozone; MP21-22; Speijer et al., 2020).

Within the formation, its lower part is composed of greenish interbedded claystones, marlstones, and limestones. The flora is rich and made up of hydrophilous taxa while the fauna is composed of lacustrine taxa (fishes and mollusks; Depape, 1926; Gaudant, 1989; Kerforne, 1915; Milon & Dangeard, 1920; Milon, 1930, 1935, 1936; Bauer et al., 2016; Lebrun et al., 2017). A small fragment of a crocodilian osteoderm was also collected. All these sedimentological and paleontological elements are consistent with a restricted and quiet lacustrine environment. The blackish color of the Upper Sapropels Formation is also an indication that the depositional environments was rich in humic materials, and the lake bottom was likely anoxic (Milon, 1930, 1935; Fig. 1C). Roots, rhizomes, and leaves are exceptionally well-preserved (Lebrun et al., 2017: pl. B, C). In addition, all known vertebrate specimens (except the osteoderm) are preserved as articulated skeletons with soft tissues (skin impressions) preserved (Lebrun et al., 2017: pl. B, C). Therefore, these laminated deposits likely represent a Konservat-Lagerstätte owing to the exquisite preservation of the fossils. The single anuran specimen was discovered within the Grand-Fours quarry (La Chaussairie) from the Upper Sapropels Formation (around 30 cm below the top of the bed).

MATERIALS AND METHODS

Institutional Abbreviations—IGR, Institut de Géologie de Rennes; **MNHN**, Muséum National d'Histoire Naturelle (Paris, France). The specimen is stored within the collection of

the geological museum of the University of Rennes under the following number: IGR 144547. Both main slab (M1) and counterpart slab (M2) are catalogued under the same number.

Reflectance Transformation Imaging (RTI)—Most bones are crushed or preserved as partial imprint and thus difficult to identify. RTI is a method that computes an "interactive specimen" in which illumination can be oriented at will (Hammer et al., 2002). This method was used with a custom-made portable light dome (same as used in Cui et al., 2022). Sets of 54 photographs under different LED sources were compiled using the RTIBuilder software. The results RTI files (see supplemental data: 10.5281/zenodo.7223828) can be opened using the RTIViewer software. Both RTIBuilder and RTIViewer are freely available at www.cultruralheritageimaging.org. This study is one of the few using RTI to study fossil vertebrate specimens.

Anatomical Comparison—Comparisons were made with the neotype of "*Rana*" *aquensis* (Piveteau, 1927), MNHN.F.AIX355 ("*Rana*" *aquensis*). Comparisons were also made with an unnumbered specimen of *Pelophylax* kl. *esculantus* from the MNHN.

Anatomical Nomenclature—The anatomical nomenclature used is that by Sanchíz (1998) for postcranial features, Roček et al (2022) for carpals, and Gómez and Turazzini (2016) for iliac features.

SYSTEMATIC PALEONTOLOGY

ANURA Duméril, 1805

NEOBATRACHIA Reig, 1958

RANOIDEA Rafinesque, 1814

RANIDAE Batsch, 1796

PELOPHYLAX Fitzinger, 1843

PELOPHYLAX KL. *ESCULENTUS* (Linnaeus, 1758)

Position of the Specimen on the Slabs

The preserved portion of the specimen is 56 mm long (anterior end of ?omosternum to distal end of femora) on a 101x107 mm slab (M1) with its 69x63 mm partial counterpart (M2). The slab (M1) preserves a majority of the fossil, from base of the cranium to the femora (Fig. 2A, B). The partial counterpart (M2) preserves only the posterior region of the body and the hands (Fig. 2C, D). A majority of the bones are surrounded by a thin black veil interpreted as a skin impression, (see below; Fig. 2A, C). The bones of the specimen are preserved as (1) slightly crushed bony elements, (2) crushed and fragmentary bony elements; (3) imprint of the bone and (4) a mix of crushed bony element and imprint on both plates. As M1 is the main plate, the position and lateralization of the anuran skeleton are based on this slab. The imprint left by the humerus on the right side of M1 (see Fig. 2) preserves some detail distally (Fig. 2). Compared to the humeral imprint made from an extant *Pelophylax* (see Fig. S1), the fossa cubitalis and eminentia capitata are preserved as an imprint. Thus, we interpret the humeral imprint on IGR 144547 as visible in ventral view on M1. Hence, when the bone is preserved on M1, it is visible in dorsal view. Thus, IGR 144547 present an anuran specimen in dorsal view on M1, and in ventral view on M2. When only the imprint of the bone is preserved, it is visible in ventral view (on M1, opposite for M2). Hence, on M1, the left side of the specimen is visible on the left region of the plate, while it is preserved on the right region of the plate on M2.

Soft Tissues

The soft tissues surround most of the bones, except for the skull and part of the tibiofibula on both M1 and M2 (Fig. 2A, C). Although it is not well defined in most region, the preservation around the hands, femora, and cloacal region allows interpretation of this feature

as skin impressions. The body shape is hard to define on the torso, although it seems to widen at midlength (Fig. 2A). The body outline then narrows towards the cloacal region.

The skin around the shoulder and forelimb is poorly preserved. Skin around the hands is well preserved on both M1 and M2 (Fig. 2A, C). The left hand preserves the shape of the flesh around the digits, and the skin narrows towards the last phalanx of the digits. Around the femora, the skin is wider near its proximal margin, and progressively narrows distally until the end of both femora. On M2, small patches of skin imprints seem preserved around the left tibiofibula (Fig. 2C, D).

Osteological Description

IGR 144547 is an anuran skeleton missing its skull, its anterior vertebrae, most of the left elements of its pectoral girdle and most of its hindlimbs (Fig. 3). The skeleton is mostly articulated, but poorly preserved, in particular in the main body region (Figs. 2, 3).

Vertebral Column

General Comments—All vertebrae are badly preserved. Most of them are hollowed out, with only faint traces of centra and transverse processes preserved. Where bone is still present, the vertebrae are exposed in dorsal view, but the neural region has been crushed or eroded on all vertebrae, leaving the centrum exposed (Fig. 4). Presacral and sacral vertebrae are only preserved on M1. A single sacral vertebra is identified, while five presacral vertebrae are preserved. The atlas, second and third vertebrae are not preserved, due to a missing piece on M1 (Fig. 2A). IGR 144547 likely possessed eight presacral vertebrae.

Vertebra IV—The centrum and transverse processes of the fourth vertebra are preserved as crushed bone in dorsal view. The centrum is broken anteriorly. It connects posteriorly with the fifth vertebra and on its right lateral side with the sternum (Fig. 4A, B).

The base of the left transverse process shows that the processes extend slightly posteriorly. They seem to expand distally (Fig. 4B).

Vertebra V—The centrum of the fifth vertebra is preserved as crushed bone in dorsal view. It bears an anterior cotyle and a posterior condyle. It connects anteriorly to the fourth vertebra and posteriorly to the sixth vertebra. A broken transverse process might be preserved on the left lateral side of the centrum (Fig. 4B). It seems posteriorly oriented, like the transverse processes of the seventh vertebra (see below), but it is broken from the centrum and we cannot assess if it is its in-situ orientation.

Vertebra VI—Only the procoelous centrum of the sixth vertebra is preserved as crushed bone in dorsal view. It connects anteriorly to the fifth vertebra and posteriorly to the seventh vertebra. No transverse processes are preserved.

Vertebra VII— This vertebra has the longest preserved centrum (2.2 mm). It bears anterior cotyle and a posterior condyle and is connected anteriorly to the sixth vertebra and posteriorly to the eighth vertebra. The transverse processes are partially preserved. They are crushed and are separated from the centrum. They are rather long and seem slightly posteriorly oriented. However, the base of the left transverse process appears to be preserved (Fig. 4A, B) and is laterally oriented.

Vertebra VIII—The last presacral is preserved throughout its centrum. Its centrum is short (1.4 mm). It bears an anterior and a posterior cotyle. An amphicoelous posterior presacral vertebra, with the remaining presacrals procoelous is diagnostic for a diplasiocoelous vertebral column. A small remnant of the left transverse process is preserved on M1 (Fig. 4A, B). It shows that the processes were straight and extended laterally.

Sacral vertebra—The sacral vertebra is only preserved on M1. Its centrum is preserved as a hollow structure exposed dorsally (Fig. 4A, B). Nevertheless, its shows that an anterior condyle and two posterior condyles are present. The centrum is short (2mm) and wider than longer (2.6 mm width). The centrum seems to widen posteriorly (Fig. 4B). Both sacral

transverse processes are preserved on M1 as imprints (in ventral view) with bone fragments. The right sacral transverse process is incomplete. The processes are oriented posterolaterally. They barely expend distally and instead are slender rod-like structures. Thus, we interpret that IGR 144547 as possessing a "Type IIA" sacrum (Emerson, 1979; Reilly & Jorgensen, 2011). The sacral vertebra possesses a small diapophyseal expansion. Both sacral processes connect distally with the ilium.

Urostyle—The urostyle is preserved on both M1 and M2. The proximal portion of the urostyle is preserved on M1 as crushed bone exposed in dorsal view on M1 and in ventral view on M2. The urostyle shaft is covered by sediment for most of its length on M1. On M2, the shaft is preserved as crushed bone (Fig. 2C). The urostyle is long (17 mm). It connects anteriorly to the sacral vertebra. Although poorly preserved, it is clear that two cotyles were present on its anterior surface. Most of the urostyle shaft is hollowed. The urostyle narrows progressively distally (Fig. 4C, D). Its distal end is crushed and covered by sediment on both M1 and M2. The urostyle seems to end slightly anterior to the acetabular region of both ilia (Fig. 2B, D). On M2, the anterior region of the urostyle is preserved as an imprint exposed dorsally, with a thin lamina of bone present medially (Fig. 4C). It suggests that a dorsal crest is present on the urostyle of IGR 144547 and extended for at least half of its length. However, we cannot assess the height of the dorsal crest, nor its total extension on the length of the urostyle.

Pectoral Girdle

Scapulae—The right scapula is preserved on M1 as an imprint with crushed bone. The left scapula is not preserved on M1. Scapulae are not preserved on M2. The scapula is elongate (7.81 mm length), with a shaft extended laterally (Fig. 5A, B). The shaft scapula expands distally, reaching its widest point at the suprascapular margin (Fig. 5B; 4.42 mm width). The latter is straight. The anterior and posterior margins are concave. Both margins lack laminae. The pars acromialis is mostly preserves as an imprint exposed in ventral view (Fig. 5A, B),

expect near the glenoid fossa. The pars acromialis is wide (3.3 mm), and part of this processus is preserved as bone exposed in dorsal view in the glenoid region (see Fig. 5B). The glenoid region is poorly preserved, with undefined crushed bony elements visible (Fig. 5B). As the specimen is exposed dorsally, it suggests that most of the bony elements form the base of the pars glenoidalis, distinct from the crushed pars acromialis (Fig. 5B). Thus, it is not possible to assess the size of the pars glenoidalis and if the latter and the pars acromialis were separated by a sinus glenoidalis.

Clavicles—Clavicles are only preserved on M1. The clavicle articulates with the scapula and humerus (forming a part of the glenoid fossa). The right clavicle is partially preserved as an imprint (exposed in ventral view; Fig. 5A), while the left clavicle is not preserved. The extremitas medialis is not preserved. Thus, it is not possible to assess if the latter articulated with the medial margin of the coracoid. The clavicle is slender and moderately developed (5.89 mm preserved). Its shaft slightly arched. The glenoid region is partially obscured by fragments of unidentified bone (Fig. 5A, B).

Coracoids—Both coracoids are preserved on M1 as imprints exposed in ventral view (Fig. 2A). The right coracoid is almost complete. It forms part of the glenoid fossa laterally, thus articulating with the clavicle and humerus. It also articulates medially with the left coracoid. The coracoid is shorter (6.64 mm) than the scapula. The processus glenoidalis widens laterally. It bears two distinct articular facets on its proximal surface. The anterior facet articulates with the clavicle and the posterior facet received the humerus. The shaft is elongated transversely and narrow. The processus epicoracoidalis is anteroposteriorly elongated. It is the widest region of the coracoid (5.3 mm). The processus is flat and bears a convex medial margin (Fig. 5B). It slightly extends anteriorly, but does not seem to form an anterior hook (as seen in *Thaumastosaurus*; Laloy et al., 2013; Lemierre et al., 2021).

Both coracoids were likely in contact medially when accounting for the connecting cartilage of the coracoids (Ecker, 1889). This is characteristic of the firmsternal condition for the pectoral girdle (sensu Cope, 1864; Boulenger, 1886).

Sternum—The sternum is preserved as a crushed bone (exposed in dorsal view) within the space left by the vertebral column on M1 (Fig. 5B). The reconstruction shows that the bone is fully ossified (Fig. 5C). The bone is elongated anteroposteriorly (4.5 mm) and hourglass-shaped. Both anterior and posterior regions are wider than the shaft and the anterior region is wider than the posterior.

Omosternum?—A small, poorly preserved element is preserved anterior to the preserved medial region of the right clavicle on M1. It is very small (2.24 mm length) and crescentic (Fig. 5A, B). It likely represents around half of a bony element. A putative reconstruction indicates the element had an inverted Y-shape (Fig. 5C). The posterior end seems connected to the extremitas medialis of the clavicle. The remaining part of the bone is a slender stylet (Fig. 5B). The position and shape of this element is incompatible with a vertebral element. Thus, we tentatively interpreted this element as an incomplete omosternum. As for the non-overlapping coracoids, the presence of an ossified omosternum is diagnostic for a firmsternal pectoral girdle (sensu Boulanger, 1886).

Pelvic Girdle

Ilia—Both ilia are preserved on M1 and M2. M1 preserves most of the distal region and shaft of the ilia as flattened bones, exposed in medial view (Fig. 2A). Both distal ends are in contact with the posterior region of the sacral apophyses. The acetabular region is only preserved as an imprint exposed in lateral view of the left ilium on M1 (Fig. 2A). On M2, the left ilium is preserved in its acetabular region with most of the bone intact and exposed in lateral view (Fig. 2B, 6B). The right ilium has been broken in two. Its distal region on M1 is crushed and separated into two halves (Fig. 2A). The shape of the displaced sediment suggests

it could have been the result of damage during the splitting of M1 and M2 by the collector. The acetabular region is displaced and covers part of the right femur and the dorsal acetabular expansion of the right ilium on M2 (Fig. 2C). This part of the right ilium is preserved as a bone exposed in medial view. The distal region of both ilia is preserved on M2 as imprints exposed in medial view. The ilium is around 19.5 mm long. It is slightly longer than the urostyle. The iliac shaft is slightly compressed laterally. The shaft bears a high dorsal crest (same height as the iliac shaft) on its whole length (Fig. 2A), as seen on M1. The dorsal protuberance ('tuber superior' in Bailon, 1999) is a large pyriform structure protruding laterally posterior to the dorsal crest (Fig. 6B, C). The supracetabular fossa is well-developed (Fig. 6B, C). The dorsal acetabular expansion is not fully preserved but seems short and oriented posteriorly (Fig. 6C). The ventral acetabular expansion has a large ventral vector (Fig; 6B, C). Its preacetabular angle is clearly acute (Fig. 6C). In medial view, there is no interiliac tubercle.

Forelimbs

Humeri—Both humeri are preserved only on M1. The proximal regions of both humeri are preserved as both crushed bone and imprint, while the remaining of the diaphysis and distal region is preserved only as an imprint exposed in ventral view. The right humerus is around 11 mm long. The proximal head of the right humerus is hard to identify, as the glenoid region is poorly preserved (Figs. 5, 7D). The proximal region of the left humerus is preserved mostly as crushed bone (exposed in dorsal view) but its outline is difficult to determine (Fig. 7A, B). No crista ventralis is preserved. If present, the crista did not extend past the mid-diaphysis (region preserved as a ventral imprint; Fig. 7C). The distal region of the right humerus is preserved as an imprint exposed ventrally. The fossa cubitalis is shallow and slightly triangular shaped (Fig. 7C, D). The fossa does not extend on the diaphysis. The eminentia capitata (humeral ball in Gómez & Turazzini, 2021) is wide and large (Fig. 7C, D). This structure is partially preserved on the left humerus as eroded bone (thus visible in dorsal view; Fig. 7A) and on the right

humerus as an imprint (visible in ventral view; Fig. 7C). The eminentia capitata is not shifted laterally from the central axis of the diaphysis. The epicondylus radialis (lateral epicondyle) is partially preserved on the right humeral imprint (Fig. 7D). It is distinct from the eminentia capitata but does not extend distally past the humeral ball (Fig. 7C, D). The epicondylus ulnaris (medial epicondyle) is not preserved, hidden by the imprint of the radioulna (Fig. 7C).

Radioulnae—Only the right radioulna is preserved for its entire length on M1. Most of it is preserved as a ventrally exposed imprint (Fig. 7C). Only the distal region of the left radioulna is preserved on M1 as a ventrally exposed imprint. The distalmost portion of the left radioulna is preserved mostly as crushed bone on M2. The right radioulna (around 9 mm) is slightly shorter than the humerus (around 80% of total humeral length). The proximal region is articulated with the distal region of the humerus (Fig. 7C). The remaining imprint of the articulation did not preserve the shape of the proximal region. The diaphysis widens distally (Fig. 7D). It reaches its widest point at the level of the distal margin. Although badly crushed on M2, the presence of a shallow groove at mid-width is discernible (Fig. 7D). This groove allowed to discern both radial and ulnar articulation facets with the carpals (Fig. 7D).

Hands—Both hands are not fully preserved. The left hand preserves most elements, except for one phalanx on both M1 and M2 (Fig. 2A, C). Four digits are visible, with the following phalanx formula : 2–2–3–3. The right hand is poorly preserved on M1 (Fig. 2A)

Carpals—All carpals are preserved on both hands (Fig. 2A). Unfortunately, they are poorly preserved as crushed bones exposed in dorsal view. However, most of their shape has been preserved as imprint. Left and right carpals are preserved on M1 (Fig. 2A). Only the left carpals are preserved on M2 (Fig. 2C). The description is based on carpals from the left hand, preserved in dorsal view (see Fig. 8A). The carpals of the left hand seem preserved in anatomical position. Two rows are preserved.

The proximal row preserves three bones (left to right): the ulnare, radiale, and distal radiale (Fig. 8B). The ulnare (left lateral imprint) is roughly ellipsoid, slightly elongated

transversely (Fig. 8B). It articulates with the ulnare part of the articular surface of the radioulna, the radiale, and the distal ulnare (Fig. 8B). Three distinct articular facets are present on the ulnare. The posteromedial region of this element is slight protruding towards the radiale (Fig. 8B). This protrusion is interpreted as the fused intermedium (following Fabrezi and Alberch, 1996).

The radiale is the largest (both in width and length) of the proximal carpals. Its shape is difficult to discern but seems circular (Fig. 8). It articulates with the radial part of the articular surface of the radioulna, the ulnare, the distal radial element, and the distal carpalia III and IV (Fig. 8B). All four articular facets are concave (Fig. 8B).

The distal radial element is free. It articulates with the radiale, the distal carpale II, and the prepollex (Fig. 8B). The distal radial element is crescent-shaped, and its lateral margin is concave (Fig. 8B). Its proximal margin seems close to the radial (Fig. 8B). This is likely an artefact of preservation, as this region is difficult to visualize (Fig. 8A).

The distal row has three bones preserved: the distal carpal element (fused distal carpalia III, IV and ulnare element), the distal carpal II, and the prepollex (Fig. 8A). Distal carpalia III, IV and ulnare element (distal carpale V of Fabrezi & Alberch, 1996) are all fused into a single large bone (Fig. 8B). It contacts the ulnare, radiale, metacarpals III-V and the distal carpale II (Fig. 8B). The anterior margin bears two distinct articular surfaces for the ulnare and radiale (Fig. 8B). There is no indication that distinct articular facets are present on the posterior margin (Fig. 8B). The bone is crescentic, with a convex posterior margin (Fig. 8B).

Distal carpale II is a small circular element (Fig. 8B). It contacts the distal radial element, the prepollex, the distal carpal element, and the metacarpal II (Fig. 8B).

The prepollex is barely evident. Most, if not all, neobatrachians possess a prepollex composed of two distinct bones (Fabrezi & Barg, 2001). Unfortunately, only a single imprint is visible on the left hand of IGR 144547 (Fig. 8A). On its right hand this region is not preserved (Fig. 2B). As the two bones of the prepollex are often in contact (see Roček et al., 2022:fig.

2L) it is possible that they left a single imprint. The prepollex is small and triangular (Fig. 8B). It contacts the distal radial element, the distal carpale II, and the metacarpal II (Fig. 8B).

Metacarpals—Metacarpals II-V are all preserved on both hands on M1 (Fig. 2A, C). Shallow imprints of the left metacarpals are preserved on M2 (Fig. 2B). The right metacarpals are poorly preserved and poorly defined (Fig. 2A). Metacarpal II contacts the distal carpale II, and prepollex proximally and the phalanx I of II distally (Fig. 8B). It is one of the longest metacarpals (4,7 mm). Its proximal head is wider than its distal head. Both proximal and distal articular facet seems flat and straight (Fig. 8B). The bone is elongated, with a rather narrow diaphysis (Fig. 8B). Metacarpal III is shorter (4.5 mm) than metacarpal II. It contacts the distal carpale III proximally and the phalanx I of digit III distally. It is preserved with bone, with both proximal and distal heads are broken, while the diaphysis seems complete (Fig. 8A). As for metacarpal II, the diaphysis is elongated and narrow. The proximal head is wider than the distal head (Fig. 8B). The proximal and distal articular facets are flat and straight (Fig. 8B). Metacarpal IV is as long as metacarpal III (4.5 mm). It contacts the distal carpale IV proximally and the phalanx I of digit IV distally. As for metacarpal III, its distal and proximal heads are broken, and most of the diaphysis is broken as well (Fig. 8A). The proximal end bears a flat articular surface (Fig. 8B). The distal head is too damaged to assess the shape of its articular facet (Fig. 8B).

Metacarpal V is as long as metacarpal II (4.8 mm). It contacts the distal ulnare element proximally and the phalanx I of digit V distally. It is complete (Fig. 8B) . Its proximal head is wider than its distal head. The articular facet of the proximal head is concave (Fig. 8B). The articular facet of the distal head is flat.

Phalanges—Phalanges are only preserved on the left hand, on both M1 and M2. Phalanx I is preserved on all digits (Fig. 8A). It is preserved as an imprint on digits II and V, and as a complete bone on digits III and IV. On digits II and IV, the phalanx is elongate (3.3 and 3.4 mm). On digit II, it is only preserved as a poorly defined imprint (Fig. 8A). On digit

IV, the preservation shows that the proximal head is wider than its distal head (Fig. 8B). Both articular facets are flat. On digits III and V, phalanx I is shorter (2.8 and 2.4 mm), and the proximal and distal heads are of the same width (Fig. 8B).

Phalanx II is also preserved on all digits. It is preserved as an imprint on digits II and V, and as a complete bone on digits III and IV. For digits II and III, it is the terminal phalanx. It is very short (1.5 mm). The phalanx narrows distally, before ending into a knob (Fig. 8B). On digits IV and V, the phalanx II is connected distally to the phalanx III (Fig. 9B). It is shorter than the phalanx I (2.6 and 2.2 respectively mm). Both proximal and distal heads are not distinct from the diaphysis.

Phalanx III is preserved on digit IV only as an imprint (Fig. 8A). It is the terminal phalanx for digits IV and V (missing on IGR 144547). It is identical to the terminal phalanx of digits II and III. It is short (1.5 mm) and bears a knob on its distal end (Fig. 8B).

Hindlimbs

Femora—Both femora are preserved on M1 and M2. The left femur is incomplete on M2. Both femora are preserved as a well-delimited imprints (exposed in ventral view) with remnants of bone (Figs. 2A, C; 11A). Femora are long (22.1 mm) and slender. The proximal head of the femur is badly preserved and mostly crushed near the acetabulum (Fig. 9B). No crest nor flange is visible on its lateral and medial margines (Fig. 9B). The femur is slightly sigmoid (S-shaped). No crest is visible on the femur shaft.

Tibiofibulae—Only the left tibiofibula is incompletely preserved on both M1 and M2. The proximal region is preserved as an uncrushed bone, while the diaphysis is mostly preserved as an imprint (exposed in ventral view). The distal region is not preserved (Fig. 9A, B). The proximal head bears a shallow groove mid-width. This groove marks the separation between the fused tibia and fibula (Fig. 9A, B). The tibiofibula is long (14 mm in length) and

straight. Slightly more than half of the tibiofibula appears to be preserved. Thus, the complete tibiofibula is probably slightly longer than the femur.

DISCUSSION

Taxonomic Attribution

Comparison to Extant European Anurans—The presence of a bicondylar sacro-urostylar articulation, a firmsternal pectoral girdle and a diplasiocoelous vertebral column are diagnostic for ranoid (Frost et al., 2006). Within Ranoidea, only natatanuran taxa are known in Europe in the Cenozoic (Roček, 2013). Furthermore, an ossified omosternum, if present, is considered a natatanuran synapomorphy (Frost et al., 2006; Lemierre et al., 2021). Within this clade, only Ranidae are known in Europe from the Oligocene (Sanchíz, 1998; Roček, 2013; Rage, 2016; Vasilyan, 2018). IGR144547 is similar to Ranidae in the following features: slender rod-like sacral apophyses, the eminentia capitata of the humerus is not shifted from the central axis of the humeral diaphysis and there is no crest on the femur.

Cenozoic and extant ranids from Western Europe have been only referred to two genera, *Rana* and *Pelophylax* (Duellman & Trueb, 1994; Sanchíz, 1998; Roček, 2013; Rage, 2016). During the twentieth and early twenty-first centuries, most authors considered the two genera synonymous (with *Pelophylax* sometimes considered a subgenus of *Rana*; Frost et al., 2006). In consequence, almost all known Cenozoic ranid from Europe were described as "*Rana*" (Sanchíz, 1998), regardless of their affinity towards the green water frogs (*Pelophylax* spp.) or brown water frogs (*Rana* spp.). In addition, osteological differences between extant European ranid and their Cenozoic counterpart are sometimes hard to find (Sanchíz, 1998). In addition, most of the European *Pelophylax* are grouped into the *Pelophylax* kl. *esculentus*, as hybridization is possible between species included into this complex (Lymberakis et al., 2007), and few (if any) osteological differences exists (Crochet et al., 1995). Thus, most of the taxa

erected since the nineteenth century are considered dubious (Sanchíz, 1998; Roček, 2013; Blain et al., 2023).

Osteological differences between *Pelophylax* and *Rana* are known for their postcranial elements (Sanchíz et al., 1993; Bailon, 1999) and cranial elements (Böhme, 1977; Bailon, 1999). The only element that allows a comparison is the ilium of IGR 144547, on which several character can be used to differentiate *Rana* and *Pelophylax* (Sanchiz et al., 1993; Bailon, 1999). IGR 144547 shares with *Pelophylax* kl. *Esculentus*: a large pyriform-shaped dorsal protuberance (Sanchíz et al., 1993; Bailon, 1999), a well-developed supracetabular fossa ('dorsal preacetabular fossa' in Sanchíz et al., 1993), a high dorsal crest anterior to the dorsal protuberance (Sanchíz et al., 1993); a high angle between the dorsal protuberance and the iliac shaft (~52° in IGR 144547; Sanchíz et al., 1993), and a small preacetabular zone (Sanchíz et al., 1993). Thus, we assign IGR 144547 to the genus *Pelophylax*, as a member of the complex *Pelophylax* kl. *esculentus*. Unfortunately, there is no current diagnostic apomorphies on the ilium between the different European species *Pelophylax* that would allow a more precise taxonomic assignment (Blain et al., 2015).

***Pelophylax* in the Oligocene of France**—As mentioned above, all extinct ranids from the Oligocene of Europe were described as *Rana* until recently. Thus, the most complete Oligocene ranid, "*Rana*" *aquensis* Coquand, 1845 has been referred to *Pelophylax* in the last decades (Sanchíz, 1998) on the basis of a similar osteology to *Pelophylax esculentus* (Sanchíz, 1998). However, there has not been any formal assignment to the genus, and the taxonomic validity of the taxon (i.e, as distinct from extant *Pelophylax* species placed under the *Pelophylax* kl. *esculentus*) has yet to be established (Sanchíz, 1998).

"*Rana*" *aquensis* is known by several subcomplete articulated specimens (Fig. 12A; Piveteau, 1927: fig. 4) from the late Oligocene of Southern France (Coquand, 1845; Piveteau, 1927; Sanchíz, 1998; Gaudant et al., 2018). The neotype (MNHN.F.AIX355) of "*Rana*" *aquensis* should be referred to the genus *Pelophylax* on the following features: a high and well-

developed dorsal crest on the ilium (Sanchiz et al., 1993; Bailon, 1999), a dorsal protuberance pyriform well-developed (Sanchíz et al., 1993), and a high angle (~42°) between the dorsal protuberance and the iliac shaft (Sanchíz et al., 1993; Bailon, 1999). Thus, we consider that all specimens assigned to "*Rana*" *aquensis* should be referred to the genus *Pelophylax*. However, we refrain from assessing the validity of *Pelophylax aquensis*, as this is beyond the scope of the study. *Pelophylax aquensis* has been considered closely related to the Miocene "*Rana*" *meriani* (Piveteau, 1927). Furthermore, a recent redescription of *Pelophylax pueyoi* (Blain et al., 2023) mentioned that the latter taxon (*P. peuyoi*) could be a subjective junior synonym of the Lower Miocene "*Rana*" *meriani* Meyer, 1852 (Meyer, 1860). Thus, a complete revision of the Oligo-Miocene *Pelophylax* is needed to assess if they represent distinct taxa, and if they could be differentiated from extant *Pelophylax* taxa.

Comparison of IGR 144547 to *Pelophylax aquensis*— IGR 144547 resembles *Pelophylax aquensis* in features of the ilium, that are diagnostic for *Pelophylax* kl. *esculentus*. The pectoral girdle of *Pelophylax aquensis* is poorly preserved (Piveteau, 1927), with only the cleithrum ("omoplate" in Piveteau, 1927) mentioned. Other specimens assigned to *P. aquensis* are known but have not been described (A.L pers. obs). Thus, IGR 144547 does not differ from *Pelophylax aquensis*, but it cannot be distinguished from extant European *Pelophylax*. Hence, we refrain from any generic assignment for *Pelophylax aquensis*.

Paleobiogeography

The palearctic water frog *Pelophylax* ranges throughout Europe and Asia today (Duellman & Trueb, 1994; Chan & Brown, 2017). The divergence between the western (Europe) and eastern (Asia) lineages of *Pelophylax* has been estimated to have occurred around 35 Ma (Chan & Brown, 2017). The genus then spread throughout Europe and underwent a diversification event during the last 15 Ma (Lymberakis et al., 2007). However, the early diversification of the genus is almost unknown, as a single occurrence has been reported from

the early Oligocene of Germany (MP22; Sanchíz et al., 1993) and the genus is currently absent from the early Oligocene sites of the Quercy Phosphorites (Rage, 2016). The attribution of IGR 144547 to *Pelophylax* and its geographical location, in northwestern France is very interesting. It implies that the genus was present in northwestern Europe (from southern Germany to northwestern France) no later than 5 Ma after its arrival in Europe. Thus, *Pelophylax* apparently underwent a rapid dispersal throughout Europe during the early Oligocene. During the late Oligocene, the genus is known throughout western Europe (Roček, 2013). This wide and rapid dispersal was likely facilitated by the "Grande Coupure" extinction event. It is linked to the Eocene/Oligocene transition (33.9 Ma) when a large turnover of the amphibian fauna took place (Rage, 2016; Vasilyan, 2018), with the rise of "true" ranid (*Pelophylax*, *Rana*) in the Oligocene (Roček, 2013; Rage, 2016). Thus, *Pelophylax* benefitted of the presence of unoccupied ecological niches, and easily spread in Europe. It should be noted that this rapid and vast dispersal might also reflect a sampling bias, in particular within the Quercy Phosphorites (that represent most of anuran occurrences from western Europe during the early Oligocene; Rage, 1984, 2016). Several possible ranids have been identified (Rage, 1984, 2016) in the Quercy (MP22-23; Rage, 2016), but have not been studied since *Rana* and *Pelophylax* became accepted as separated genera.

CONCLUSION

In conclusion, IGR 144547 represents one of the oldest known members of the European *Pelophylax* kl. *esculentus*, and the oldest articulated specimen of *Pelophylax* identified. We also suggest that *'Rana' aquensis* should be included within *Pelophylax* kl. *esculentus*. IGR 144547 resembles the holotype of *Pelophylax aquensis*, but a complete revision of this taxon must be made before any assignment can be proposed. Our specimen represents the first occurrence of *Pelophylax* in the early Oligocene of France. This occurrence

suggests a rapid dispersal of *Pelophylax* throughout western Europe during the Oligocene. This opportunistic frog genus likely benefited from unoccupied ecological niches and the decrease in anuran diversity following the "Grande Coupure".

ACKNOWLEDGEMENTS

We wanted to thank O. Béthoux (CR2P, MNHN) for the access and loan of the portable light dome and formation on the use of the RTI softwares, V. Buffa (CR2P, MNHN) for the formation on the use of the light dome, D. Germain (CR2P, MNHN) for access to the MNHN specimens of *Pelophylax aquensis*. We also thank H.-D. Sues for his editorial work and two anonymous reviewers for their constructive reviews of the manuscript.

LITERATURE CITED

Allix, H. (1922). Note sur deux nouvelles espèces de *Lithuonella* du Tertiaire de Bretagne. *Bulletin de la Société Géologique et minéralogique de Bretagne*, *2*(2), 275–278.

Bailon, S. (1999). *Différenciation Ostéologique des Anoures (Amphibia, Anura) de France* (J. Desse & N. Desse-Berset, Eds.). Centre de Recherches Archéologiques du CNRS.

Batsch, A. J. (1796). *Umriss der gesammten Naturgeschichte* (Vol. 1). Christian Ernst Gabler.

Bauer, H., Bessin, P., Saint-Marc, P., Châteauneuf, J.-J., Bourdillon, C., Wyns, R., & Guillocheau, F. (2016). The Cenozoic history of the Armorican Massif: New insights from the deep CDB1 borehole (Rennes Basin, France). *Comptes Rendus Geoscience*, *348*(5), 387–397.

Blain, H.-A., Lózano-Fernández, I., & Böhme, G. (2015). Variation in the ilium of central European water frogs *Pelophylax* (Amphibia, Ranidae) and its implications for species-level identification of fragmentary anuran fossils. *Zoological Studies*, *54*(5), 1–9.

Blain, H.-A., Přikryl, T., Moreno-Ribas, E., & Ignacio Canudo, J. (2023). The first discovery of in situ *Pelophylax pueyoi* (Amphibia Anura) from the Late Miocene of Libros Konservat-Lagerstatte (Teruel, Spain). *Journal of Vertebrate Paleontology*, e2161410.

Böhme, G. (1977). Zur Bestimmung Anuren Europas an Hand von Skelettelementen. *Wissenschaftliche Zeitschrift Der Humboldt-Universität Zu Berli, Math-Nat. R.*, *26*, 283–299.

Boulanger, G. A. (1886). Quelques mots en réponse à la note de M. le Dr R. Blanchard sur la classification des batraciens. *Bulletin de la société zoologique de France*, *11*, 320–321.

Cahuzac, B., & Poignant, A. (1997). Essai de biozonation de l'Oligo-Miocène dans les bassins européens à l'aide des grands foraminifères néritiques. *Bulletin de La Société Géologique de France*, *168*(2), 155–169.

Chan, K. O., & Brown, R. M. (2017). Did true frogs 'dispersify'? *Biology Letters*, *13*(8), 20170299.

Cope, E. D. (1864). On the Limits and Relations of the Raniformes. *Proceedings of the Academy of Natural Sciences of Philadelphia*, *16*(4), 181–183.

Coquand, H. (1845). Sur la découverte faite dans les plâtrières d'Aix d'une grenouille fossile. *Bulletin de La Société Géologique de France*, *2*, 393–394.

Crochet, P.-A., Dubois, A., Ohler, A., & Tunner, H. (1995). *Rana* (*Pelophylax*) *ridibunda* Pallas, 1771, *Rana* (*Pelophylax*) *perezi* Seoane, 1885 and their associated klepton (Amphibia, Anura): Morphological diagnoses and description of a new taxon. *Bulletin Du Muséum National d'Histoire Naturelle, Paris, Série 4*, *17*(1–2), 11–30.

Cui, Y., Brauner, S., Schneider, J. W., & Béthoux, O. (2022). Grylloblattidan insects from Sperbersbach and Cabarz (Germany), two new early Permian and insect-rich localities. *Journal of Paleontology*, *96*(2), 355–374.

Dangead, L., & Milon, Y. (1922). Etude de la formation redonienne du Vieux-Chartres (Sud de Rennes) et de son contact avec l'Eocène. *Bulletin de La Société Géologique et Minéralogique de Bretagne*, *2*, 505–520.

Dangeard, L., & Milon, Y. (1926). Observations sur le contact du Miocène et de l'Oligocène dans la carrière des Grands-Fours, Chartres (Ille-et-Vilaine). *Bulletin de La Société Géologique et Minéralogique de Bretagne*, *7*(1–2), 74–79.

Depape, G. (1926). Végétaux fossiles des argiles à poissons de La Chaussairie et de Lormandière à Chartres (Ille-et-Vilaine). *Bulletin de La Société Géologique et Minéralogique de Bretagne*, *5*, 32–50.

Duellman, W. E., & Trueb, L. (1994). *Biology of Amphibians*. JHU Press; 702 pp.

Duméril, C. (1805). *Zoologie analytique, ou Méthode naturelle de classification des animaux, rendue plus facile à l'aide de tableaux synoptiques*. Allais, Paris, 386 pp.

Ecker, A. (1889). *The Anatomy of the Frog*. Clarendon Press.

Emerson, S. B. (1979). The ilio-sacral articulation in frogs: Form and function. *Biological Journal of the Linnean Society*, *11*(2), 153–168.

Fabrezi, M., & Alberch, P. (1996). The Carpal Elements of Anurans. *Herpetologica*, *52*(2), 188–204.

Fabrezi, M., & Barg, M. (2001). Patterns of carpal development among anuran amphibians. *Journal of Morphology*, *249*(3), 210–220.

Fitzinger, L. (1843). *Systema Reptilium. Fasciculus primus: Amblyglossae*. Fitzinger, L. (1843). Systema Reptilium. Fasciculus primus: Amblyglossae. Braumüller und Seidel.

Frost, D. R., Grant, T., Faivovich, J., Bain, R. H., Haas, A., Haddad, C. F. B., De Sá, R. O., Channing, A., Wilkinson, M., Donnellan, S. C., Raxworthy, C. J., Campbell, J. A., Blotto, B. L., Moler, P., Drewes, R. C., Nussbaum, R. A., Lynch, J. D., Green, D. M., & Wheeler, W. C. (2006). The Amphibian Tree of Life. *Bulletin of the American Museum of Natural History*, *297*, 1–291.

Gaudant, J. (1989). Découverte d'une nouvelle espèce de poissons cyprinodontiformes (*Prolebias delphinensis* nov. sp.) dans l'Oligocène du bassin de Montbrun-les-Bains (Drôme). *Géologie Méditerranéenne*, *16*(4), 355–367.

Gaudant, J., Nel, A., Nury, D., Véran, M., & Carnevale, G. (2018). The uppermost Oligocene of Aix-en-Provence (Bouches-du-Rhône, Southern France): A Cenozoic brackish subtropical Konservat-Lagerstätte, with fishes, insects and plants. *Comptes Rendus Palevol*, *17*(7), 460–478.

Gómez, R. O., & Turazzini, G. F. (2016). An overview of the ilium of anurans (Lissamphibia, Salientia), with a critical appraisal of the terminology and primary homology of main ilial features. *Journal of Vertebrate Paleontology*, *36*(1), e1030023.

Gómez, R. O., & Turazzini, G. F. (2021). The fossil record and phylogeny of South American horned frogs (Anura, Ceratophryidae). *Journal of Systematic Palaeontology*, *19*(2), 91–130.

Hammer, Ø., Bengtson, S., Malzbender, T., & Gelb, D. (2002). Imaging fossils using reflectance transformation and interactive manipulation of virtual light sources. *Palaeontologia Electronica*, *5*(4), 9.

Kerforne, F. (1915). Compte-rendu des excursions du laboratoire de Géologie de Rennes en 1915: Excusion à la Chaussairie et Lormandière (Sud de Rennes). *Bulletin de La Société Scientifique et Médicale de l'Ouest*, *24*, 65–70.

Laloy, F., Rage, J.-C., Evans, S. E., Boistel, R., Lenoir, N., & Laurin, M. (2013). A re-interpretation of the Eocene anuran *Thaumastosaurus* based on MicroCT examination of a 'mummified' specimen. *Plos One 8*, e74874

Lebesconte, P. (1879). Note stratigraphique sur le bassin tertiaire des environs de Rennes (Ille-et-Vilaine). *Bulletin de La Société Géologique de France Série 3*, *7*, 451–464.

Lebrun, P., Gendry, D., & Plaine, J. (2017). Fossiles oligocènes-miocènes des environs de Rennes. *Revue Française de Paléontologie*, *30*, 5–36.

Lemierre, A., Folie, A., Bailon, S., Robin, N., & Laurin, M. (2021). From toad to frog, a CT-based reconsideration of *Bufo servatus* , an Eocene anuran mummy from Quercy (France). *Journal of Vertebrate Paleontology*, *41*(3), e1989694.

Linnaeus, C. (1758). *Systema naturae per regna tria naturae, secundum classes, ordines, genra, species, cum characteribus, differentiis, synonymis, locis: Vol. Tomus 1* (Edition decima, reformata). Laurentius.

Lymberakis, P., Poulakakis, N., Manthalou, G., Tsigenopoulos, C. S., Magoulas, A., & Mylonas, M. (2007). Mitochondrial phylogeography of *Rana* (*Pelophylax*) populations in the Eastern Mediterranean region. *Molecular Phylogenetics and Evolution*, *44*(1), 115–125.

Meyer, D. L. (1852). Beschreibung der fossilen Decapoden, Fische, Batrachier und Säugethiere aus den tertiären Süsswassergebilden des nördlichen Böhmens. *Palaeontographica*, 1–73.

Meyer, D. L. (1860). Frösche aus Tertiär-Gebilden Deutschland's. *Palaeontographica*, *bd. 7*, 123–182.

Milon, Y. (1930). Les niveaux présumés lacustres de l'Oligocène du Sud de Rennes. *Comptes Rendus Sommaires de La Société Géologique de France*, *190*, 131–132.

Milon, Y. (1935). Les argiles noires de l'Oligocène du Bassin de Rennes. *Comptes Rendus Sommaires de La Société Géologique et Minéralogique de Bretagne*, *1*(2), 2–3.

Milon, Y. (1936). Le cycle sédimentaire Rupélien-Chattien. Les sapropèles zonés de l'Oligocène du Sud de Rennes et le rôle des fleurs d'eau. *Comptes Rendus Sommaires de La Société Géologique et Minéralogique de Bretagne*, *2*(2), 4–7.

Milon, Y., & Dangeard, L. (1920). Comptes Rendus des excursions de la Société Géologique et Minéralogique de Bretagne et de la Faculté des Sciences de Rennes. *Bulletin de La Société Géologique et Minéralogique de Bretagne*, *1*, 147–205.

Pélissié, T., Orliac, M., Antoine, P. O., Biot, V., & Escarguel, G. (2021). Beyond Eocene and Oligocene Epochs: The Causses du Quercy Geopark and the Grande Coupure. *Geoconservation Research*, *4*, 573–585.

Piveteau, J. (1927). Etudes sur quelques amphibiens et reptiles fossiles. *Annales de Paléontologie*, *16*, 1–47.

Rafinesque, C. S. (1814). Fine del prodromo d'erpetologia siciliana. *Specchio Delle Scienze, o, Giornale Enciclopedico Di Sicilia*, *2*, 102–104.

Rage, J.-C. (1984). Are the Ranidae (Anura, Amphibia) known prior to the Oligocene? *Amphibia-Reptilia*, *5*(3–4), 281–288.

Rage, J.-C. (2016). Frogs (Amphibia, Anura) from the Eocene and Oligocene of the Phosphorites du Quercy (France). An overview. *Fossil Imprint*, *72*(1–2), 53–66.

Reig, O. (1958). Proposiciones para una nueva macrosistemática de los anuros (nota preliminar). *Physis*, *21*(60), 109–118.

Reilly, S. M., & Jorgensen, M. E. (2011). The evolution of jumping in frogs: Morphological evidence for the basal anuran locomotor condition and the radiation of locomotor systems in crown group anurans. *Journal of Morphology*, *272*(2), 149–168.

Roček, Z. (2013). Mesozoic and Tertiary Anura of Laurasia. *Palaeobiodiversity and Palaeoenvironments*, *93*(4), 397–439.

Roček, Z., Dong, L., Fabrezi, M., Rong, Y., & Wang, Y. (2022). Carpus in Mesozoic anurans: The Early Cretaceous anuran *Genibatrachus* from northeastern China. *Cretaceous Research*, *129*, 104984.

Sanchíz, B. (1998). *Salientia*. (Handbuch der Paläoherpetologie, vol. 4.) Pfeil.

Sanchíz, B., Schleich, H. H., & Esteban, M. (1993). Water frogs (Ranidae) from the Oligocene of Germany. *Journal of Herpetology*, *27*(4), 486.

Speijer, R. P., Pälike, H., Hollis, C. J., Hooker, J. J., & Ogg, J. G. (2020). The Paleogene Period. In *Geologic Time Scale 2020* (pp. 1087–1140). Elsevier.

Trautmann, F., Paris, F., & Carne, A. (2000). *Notice de la carte géologique de la France à 1/50 000. Feuille Rennes (371)* [Map]. Editions du Bureau de recherches géologiques et minières.

Vasilyan, D. (2018). Eocene western European endemic genus *Thaumastosaurus*: New insights into the question "Are the Ranidae known prior to the Oligocene?" *PeerJ*, *6*, e5511.

Vasseur, G. (1881). Recherches géologiques sur les terrains tertiaires de la France occidentale: Stratigraphie. *Annales Des Sciences Géologiques*, *13*, 352–353.

SUPPLEMENTARY INFORMATION

Supplementary Data 1.docx: supplementary figure.

DATA AVAILABILITY

The data underlying this article are available in zenodo at 10.5281/zenodo.7223828.

FIGURE CAPTIONS

FIGURE 1. Location of the discovery in the Grand Four quarry (Chartres-de-Bretagne). **A**, Geological map of the Chartres-de-Bretagne basin with location of the quarry (black circle; modified from Bauer et al., 2016); **B**, Stratigraphic section of the quarry (modified from Bauer et al., 2016) with **C**, photography of the outcrop taken by Yves Milon in march 1922, note the black clay with quarrymen in the Upper Sapropels that yielded the anuran remains just above paleosols; **D**, close-up on the black clay with Yves Milon and two quarrymens, position of hammers indicates first fish remains discovered the 17th March 1922, the anuran comes from the left hammer level (photography Dangeard). Labels at the bottom are for the geological map

of **A** and black star (red in online version) represents the position of IGR 144547 within the stratigraphic log. [page width]

FIGURE 2. IGR 144547 main slab (M1) and its counterpart (M2). **A**, IGR 144547 M1, **B**, interpretative drawing of the same specimen; **C**, IGR 144547 M2 and **D**, interpretative drawing of the same specimen. Light gray areas represent regions on the specimen where bony elements could not be delimited, dark gray areas represent skin impressions, scale bars represent 10 mm. **Abbreviations**: **ca**, carpals; **cl**, clavicle; **co**, coracoid; **f**, femur; **hu**, humerus; **il**, ilium; **mtc**, metacarpal; **omst?**, putative omosternum; **phx I**, **II**, **III**, phalanx I, II, III; **rdul**, radioulna; **sc**, scapula; **tf**, tibiofibula; **ur**, urostyle. [page width]

FIGURE 3. Reconstruction of IGR 144547 in ventral view. Non-preserved elements are inferred from *Pelophylax esculentus*, gray areas represent non-preserved elements, scale bar represents 10 mm. [column width]

FIGURE 4. Vertebral elements of IGR 144547. **A**, close-up on the vertebral region of IGR 144547 on M1, **B**, interpretative drawing of the same region, **C**, close-up on the urostyle of IGR 144547 on M2 and **D**, interpretative drawing of the same region. Scale bars represent 5 mm and light gray areas represent unidentified bony elements. **Abbreviations: IV**, fourth vertebra; **V**, fifth vertebra; **VI**, sixth vertebra; **VII**, seventh vertebra; **VIII**, eighth vertebra; **il**, ilium; **stp**, sacral transverse process; **sv**, sacral vertebra; **tp**, transverse process; **ur**, urostyle. [column width]

FIGURE 5. Pectoral elements of IGR 144547. **A**, close-up on the right pectoral region of IGR 144547 on M1, **B**, interpretative drawing of the same region and **C**, reconstruction of the pectoral girdle in ventral view. Light gray area represents the glenoid region. **Abbreviations**:

cl, clavicle; **co**, coracoid; **glf**, glenoid fossa ?; **hu**, humerus; **omst?**, putative omosternum; **par**, pars acromialis; **pecd**, processus epicoracoidalis; **pgl**, pars glenoidalis; **prgl**, processus glenoidalis; **sc**, scapula; **st**, sternum. Scale bar is 5 mm. [2/3 page width]

FIGURE 6. Ilium of IGR144547. **A**, acetabular region of the left ilium exposed in lateral view on M2, **B**, proposed reconstruction of the acetabular region of the left ilium in lateral view and **C**, right ilium in exposed in medial view on M2. Scale bars represent 2 mm. **Abbreviations**: **acf**, acetabular fossa; **acr**, acetabular rim; **dae**, dorsal acetabular expansion; **dc**, dorsal crest; **dpt**, dorsal protuberance; **ish**, iliac shaft; **pz**, preacetabular zone; **saf**, supraacetabular fossa; **vae**, ventral acetabular expansion. [full page width]

FIGURE 7. Forelimbs of IG144547. **A**, left humerus on M1, **B**, interpretative drawing of the same humerus, **C**, right forelimb on M1 and **D**, interpretive drawing of the same forelimb. Light gray area represents skin impressions, scale bars represent 5 mm. **Abbreviations**: **ec**, eminentia capitata; **dia**, diaphysis; **fc**, fossa cubitalis; **recd**, epicondylus radialis.[column width]

FIGURE 8. Hand of IGR 144547. **A**, left hand on M1 and **B**, interpretative drawing of the same hand. Light gray areas represent skin impressions of the digits, scale bar represents 2 mm. **Abbreviations**: **dis rd**, distal radiale; **dist ul**, distal ulnare; **dist II**, distal carpale II; **dist III**, distal carpale III; **dist IV**, distal carpale IV; **mtc**, metacarpal; **phx I**, **II**, **III**, phalanx I, II, III; **pp**, prepollex; **rd**, radiale; **rdul**, radioulna; **ul**, ulnare. [column width]

FIGURE 9. Hindlimb of IGR 144547. **A**, right hindlimb on M1 and **B**, interpretative drawing of the same hindlimb. **Abbreviations**: **f**, femur; **tf**, tibiofibula. Dotted lines delimit skin impressions, scale bar represents 5 mm. [column width]

767

768

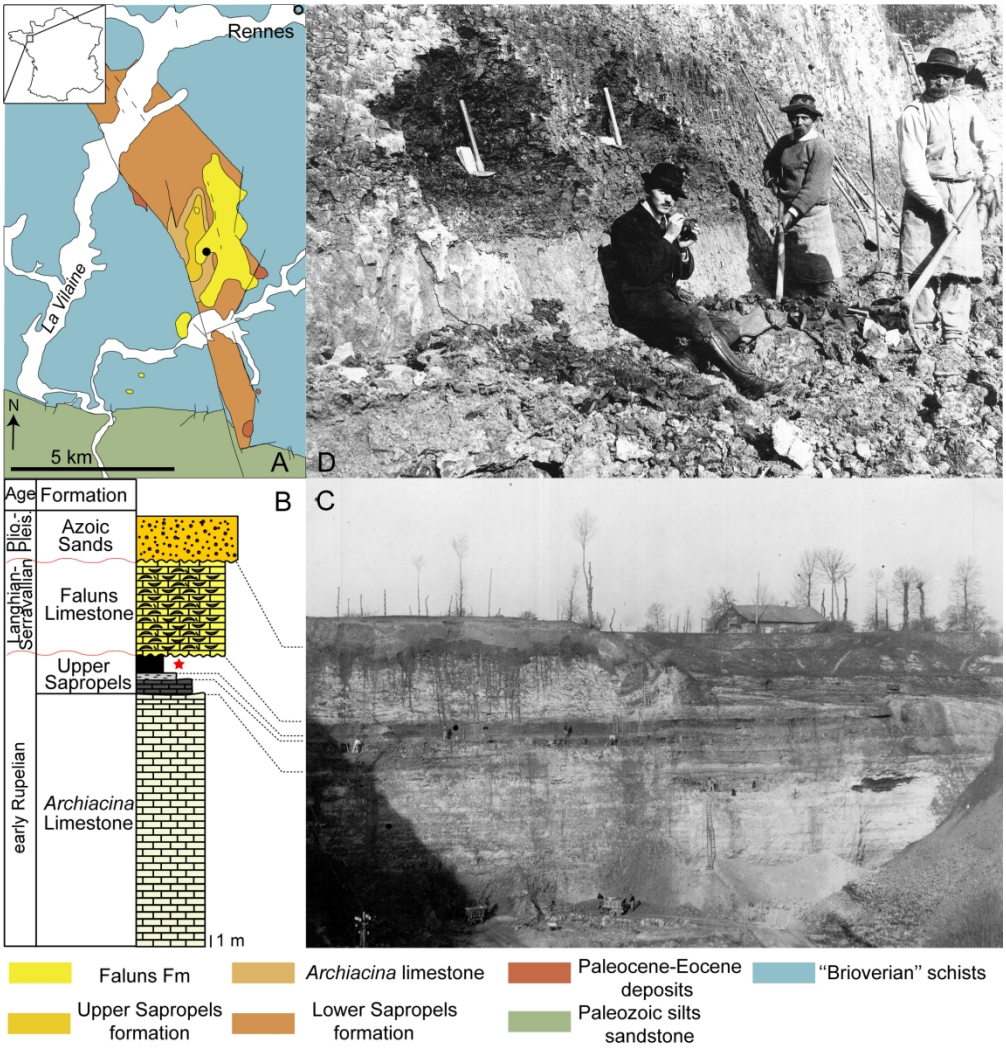

Location of the discovery in the Grand Four quarry (Chartres-de-Bretagne). **A**, Geological map of the Chartres-de-Bretagne basin with location of the quarry (black circle; modified from Bauer et al., 2016); **B**, Stratigraphic section of the quarry (modified from Bauer et al., 2016) with **C**, photography of the outcrop taken by Yves Milon in march 1922, note the black clay with quarrymen in the Upper Sapropels that yielded the anuran remains just above paleosols; **D**, close-up on the black clay with Yves Milon and two quarrymens, position of hammers indicates first fish remains discovered the 17th March 1922, the anuran comes from the left hammer level (photography Dangeard). Labels at the bottom are for the geological map of **A** and black star (red in online version) in **B** represents the position of IGR 144547 within the stratigraphic log.

182x190mm (300 x 300 DPI)

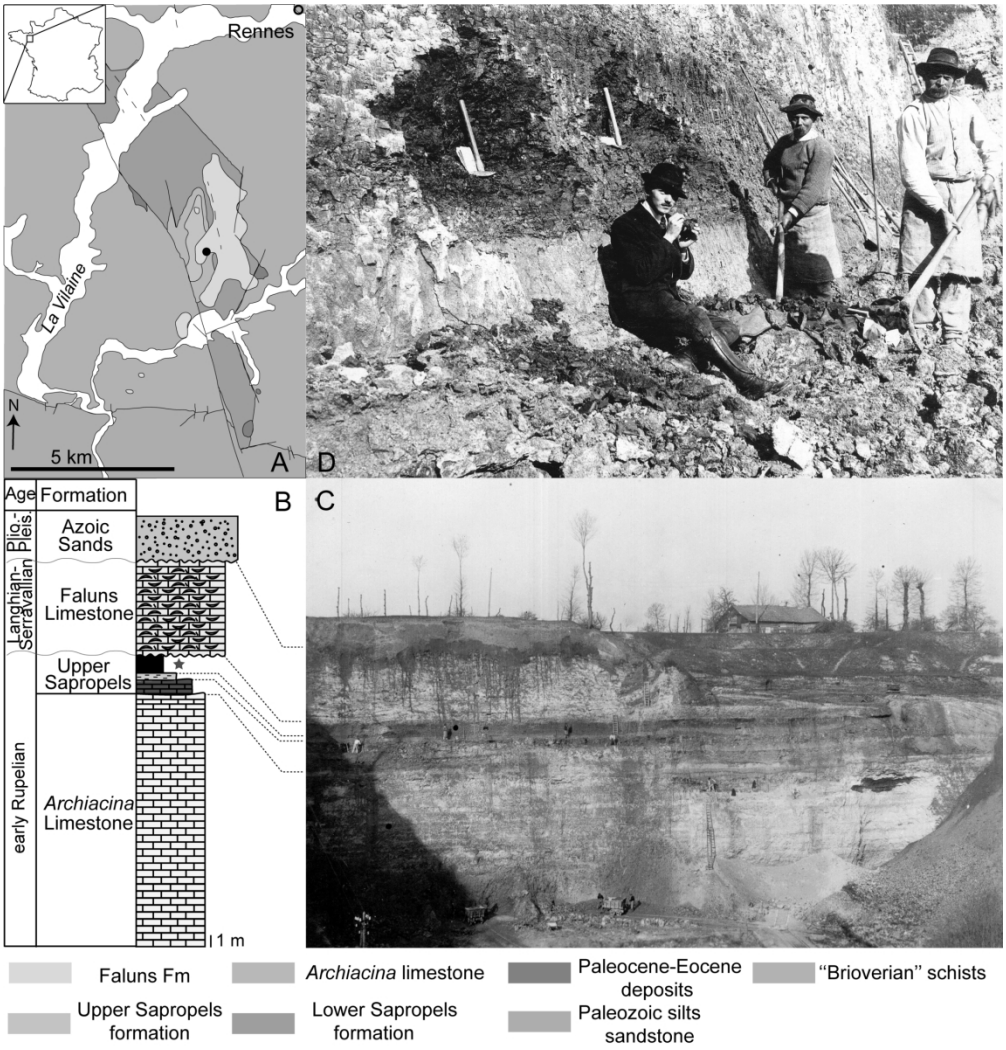

Location of the discovery in the Grand Four quarry (Chartres-de-Bretagne). **A**, Geological map of the Chartres-de-Bretagne basin with location of the quarry (black circle; modified from Bauer et al., 2016); **B**, Stratigraphic section of the quarry (modified from Bauer et al., 2016) with **C**, photography of the outcrop taken by Yves Milon in march 1922, note the black clay with quarrymen in the Upper Sapropels that yielded the anuran remains just above paleosols; **D**, close-up on the black clay with Yves Milon and two quarrymens, position of hammers indicates first fish remains discovered the 17th March 1922, the anuran comes from the left hammer level (photography Dangeard). Labels at the bottom are for the geological map of **A** and black star (red in online version) in **B** represents the position of IGR 144547 within the stratigraphic log.

182x190mm (300 x 300 DPI)

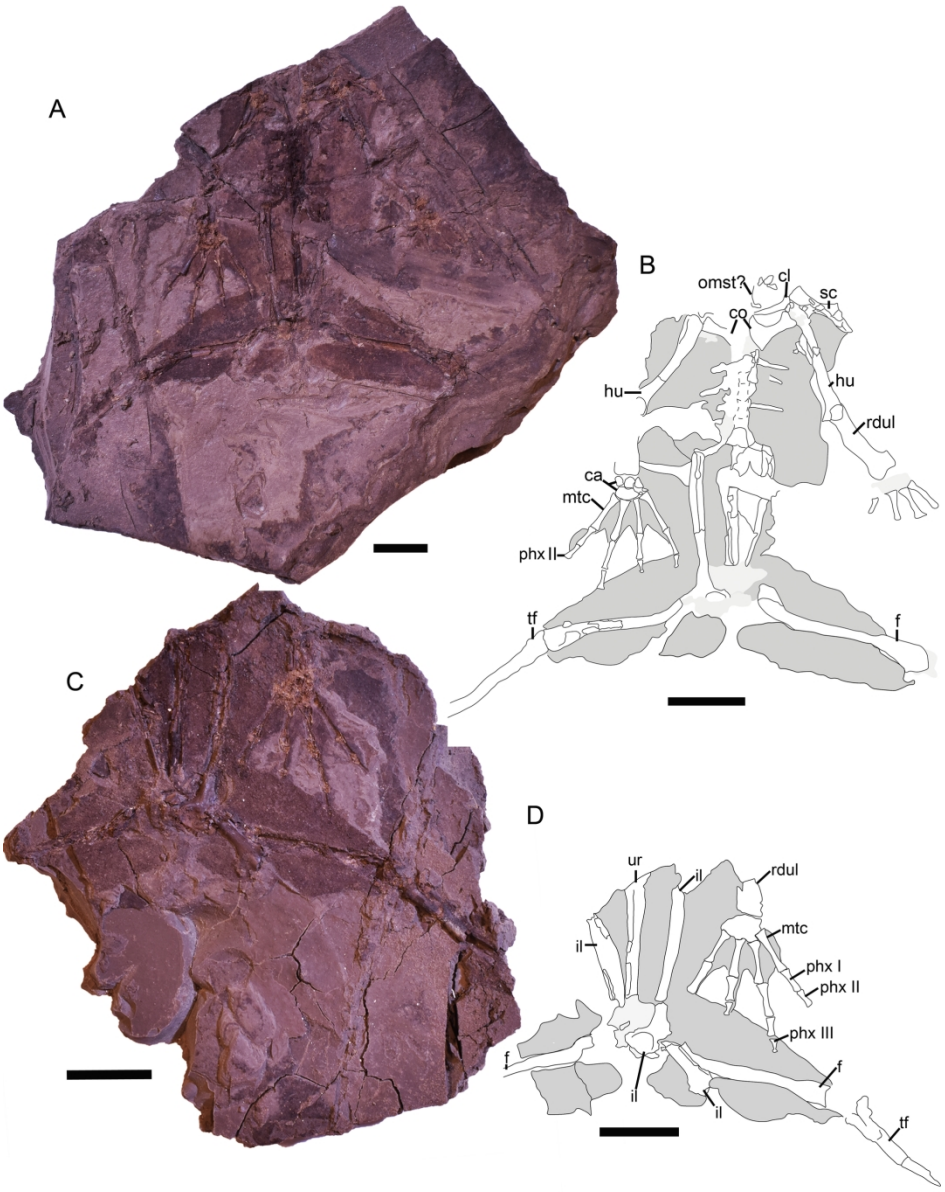

IGR 144547 and its counterpart. **A**, IGR 144547 M1, **B**, interpretative drawing of the same specimen; **C**, IGR 144547 M2 and **D**, interpretative drawing of the same specimen. Light gray areas represent regions on the specimen where bony elements could not be delimited, dark gray areas represent skin impressions regions, scale bars represent 10 mm. **Abbreviations**: **ca**, carpals; **cl**, clavicle; **co**, coracoid; **f**, femur; **hu**, humerus; **il**, ilium; **mtc**, metacarpal; **omst?**, putative omosternum; **phx I**, **II**, **III**, phalanx I, II, III; **rdul**, radioulna; **sc**, scapula; **tf**, tibiofibula; **ur**, urostyle.

182x232mm (300 x 300 DPI)

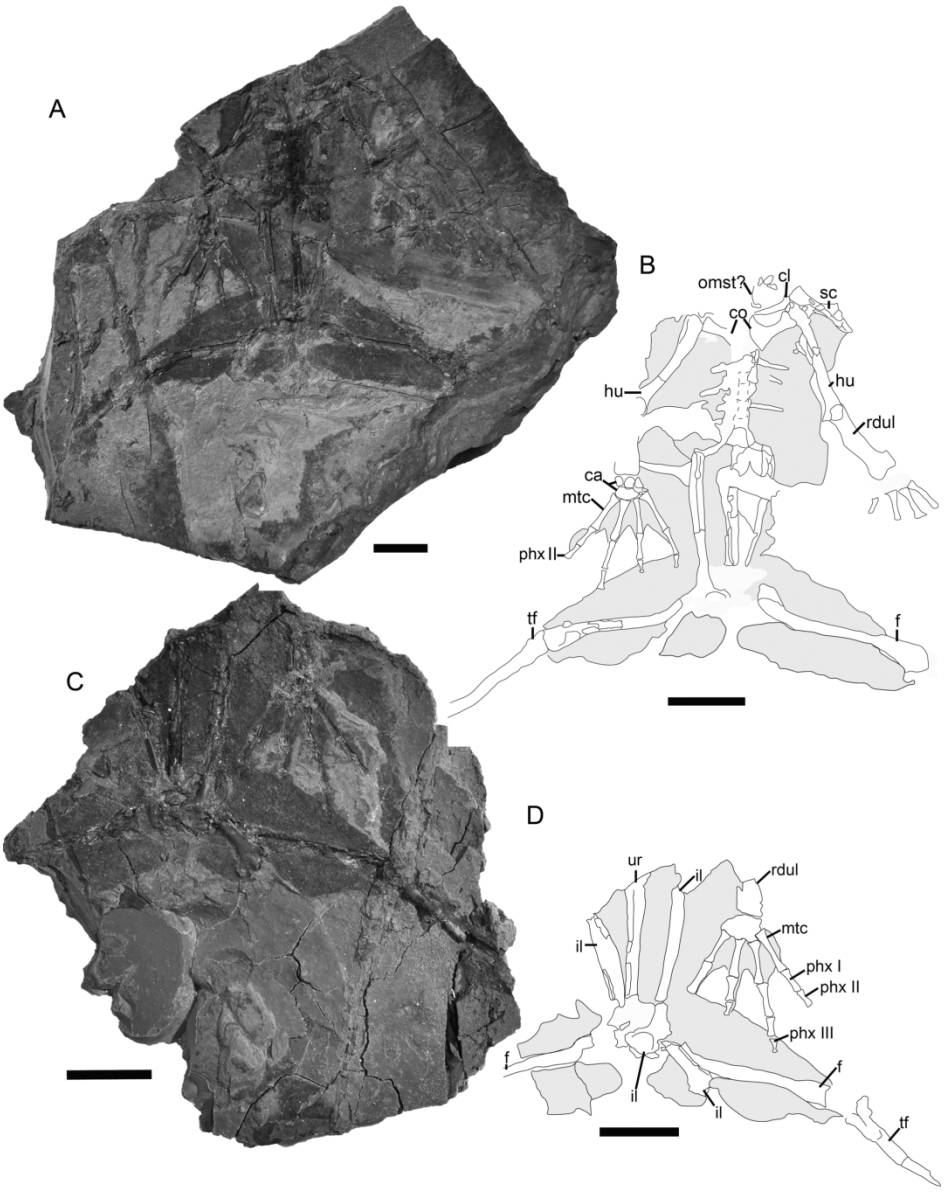

IGR 144547 and its counterpart. **A**, IGR 144547 M1, **B**, interpretative drawing of the same specimen; **C**, IGR 144547 M2 and **D**, interpretative drawing of the same specimen. Light gray areas represent regions on the specimen where bony elements could not be delimited, dark gray areas represent skin impressions regions, scale bars represent 10 mm. **Abbreviations**: **ca**, carpals; **cl**, clavicle; **co**, coracoid; **f**, femur; **hu**, humerus; **il**, ilium; **mtc**, metacarpal; **omst?**, putative omosternum; **phx I**, **II**, **III**, phalanx I, II, III; **rdul**, radioulna; **sc**, scapula; **tf**, tibiofibula; **ur**, urostyle.

182x232mm (300 x 300 DPI)

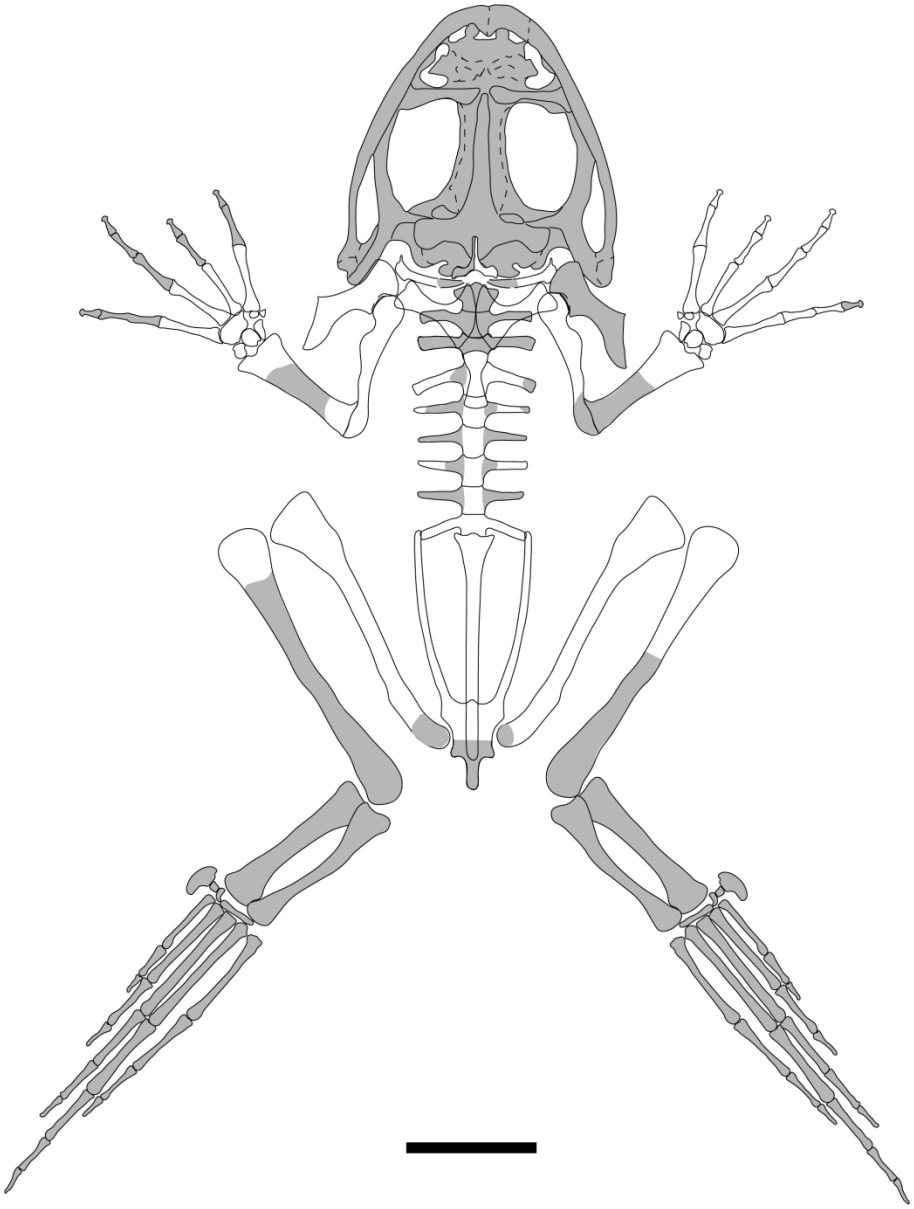

Reconstruction of IGR 144547 in ventral view. Non-preserved elements are inferred from *Pelophylax esculentus*, gray areas represent non-preserved elements, scale bar represents 10 mm.

88x116mm (600 x 600 DPI)

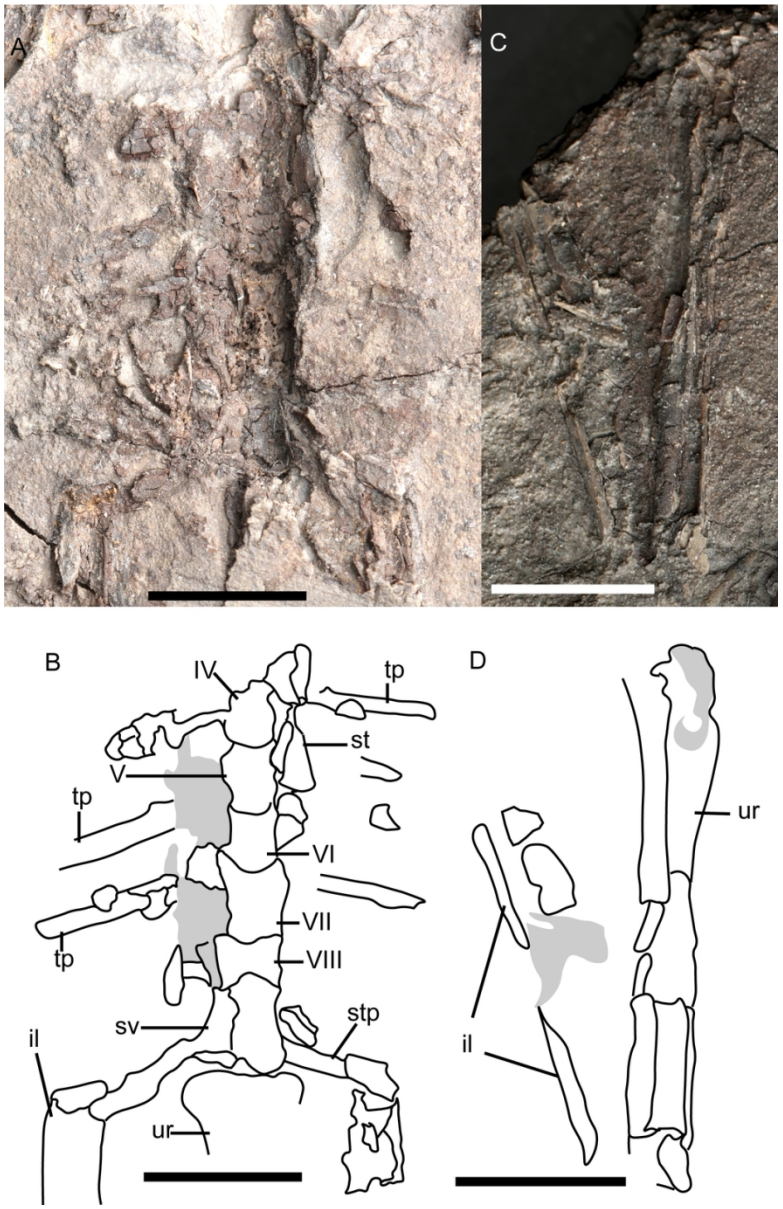

Vertebral elements of IGR 144547. **A**, close-up on the vertebral region of IGR 144547 on M1, **B**, interpretative drawing of the same region, **C**, close-up on the urostyle of IGR 144547 on M2 and **D**, interpretative drawing of the same region. Scale bars represent 5 mm and light grey areas represent unidentified bony elements. **Abbreviations**: **IV**, fourth vertebra; **V**, fifth vertebra; **VI**, sixth vertebra; **VII**, seventh vertebra; **VIII**, eighth vertebra; **il**, ilum; **stp**, sacral transverse process; **sv**, sacral vertebra; **tp**, transverse process; **ur**, urostyle.

88x136mm (300 x 300 DPI)

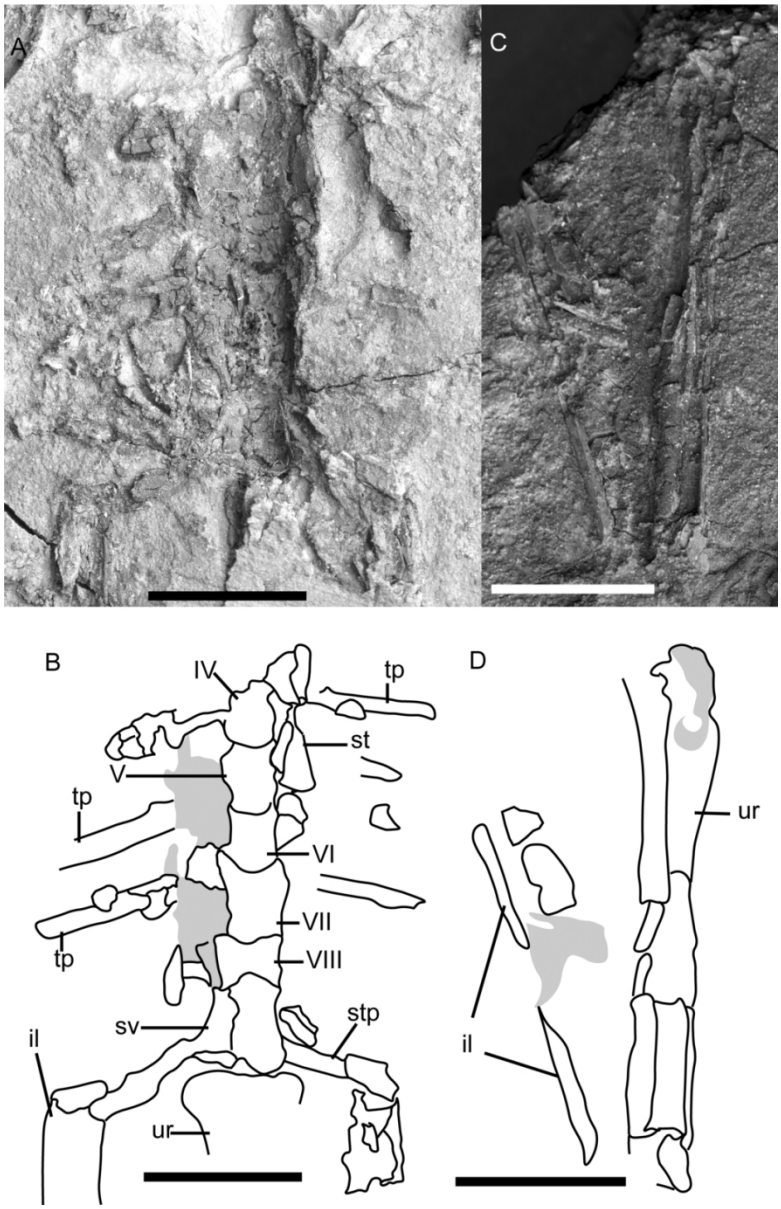

Vertebral elements of IGR 144547. **A**, close-up on the vertebral region of IGR 144547 on M1, **B**, interpretative drawing of the same region, **C**, close-up on the urostyle of IGR 144547 on M2 and **D**, interpretative drawing of the same region. Scale bars represent 5 mm and light grey areas represent unidentified bony elements. **Abbreviations**: **IV**, fourth vertebra; **V**, fifth vertebra; **VI**, sixth vertebra; **VII**, seventh vertebra; **VIII**, eighth vertebra; **il**, ilum; **stp**, sacral transverse process; **sv**, sacral vertebra; **tp**, transverse process; **ur**, urostyle.

88x136mm (300 x 300 DPI)

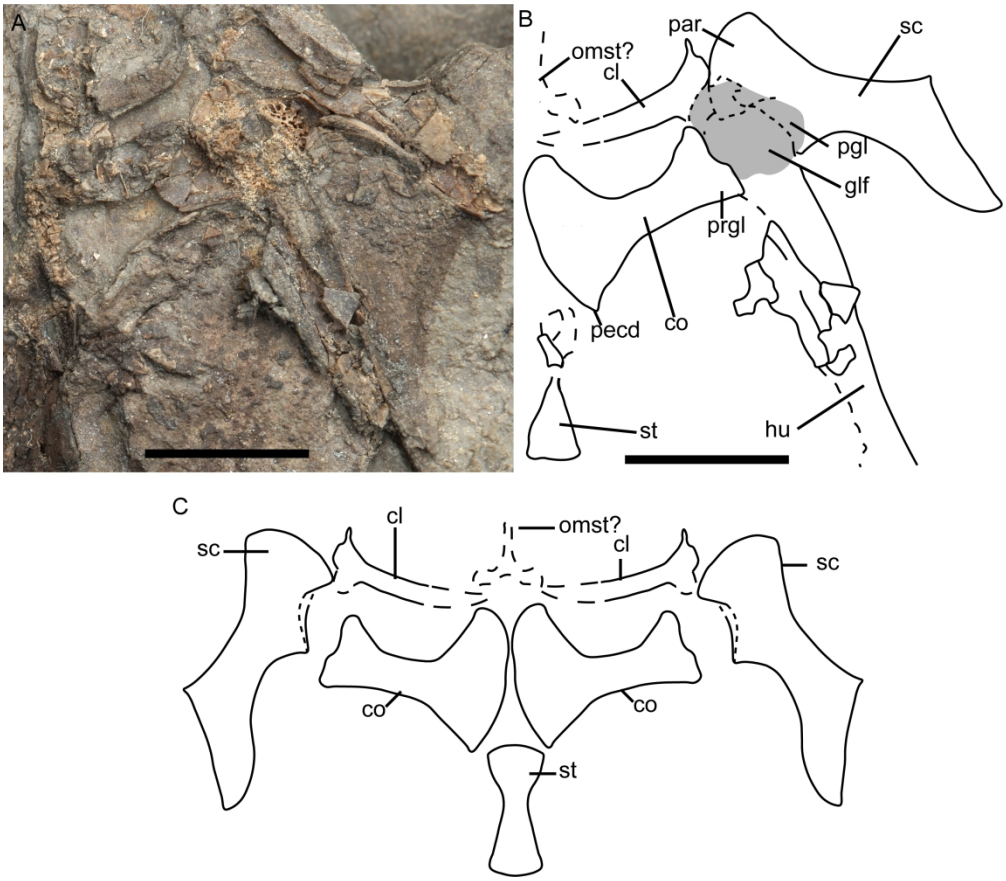

Pectoral elements of IGR 144547. **A**, close-up on the right pectoral region of IGR 144547 on M1, **B**, interpretative drawing of the same region and **C**, reconstruction of the pectoral girdle in ventral view. Light gray area represents the glenoid region. . **Abbreviations**: **cl**, clavicle; **co**, coracoid; **glf**, glenoid fossa?; **hu**, humerus; **omst?**, putative omosternum; **par**, pars acromialis; **pecd**, processus epicoracoidalis; **pgl**, pars glenoidalis; **prgl**, processus glenoidalis; **sc**, scapula; **st**, sternum. Scale bar is 5 mm.

122x106mm (600 x 600 DPI)

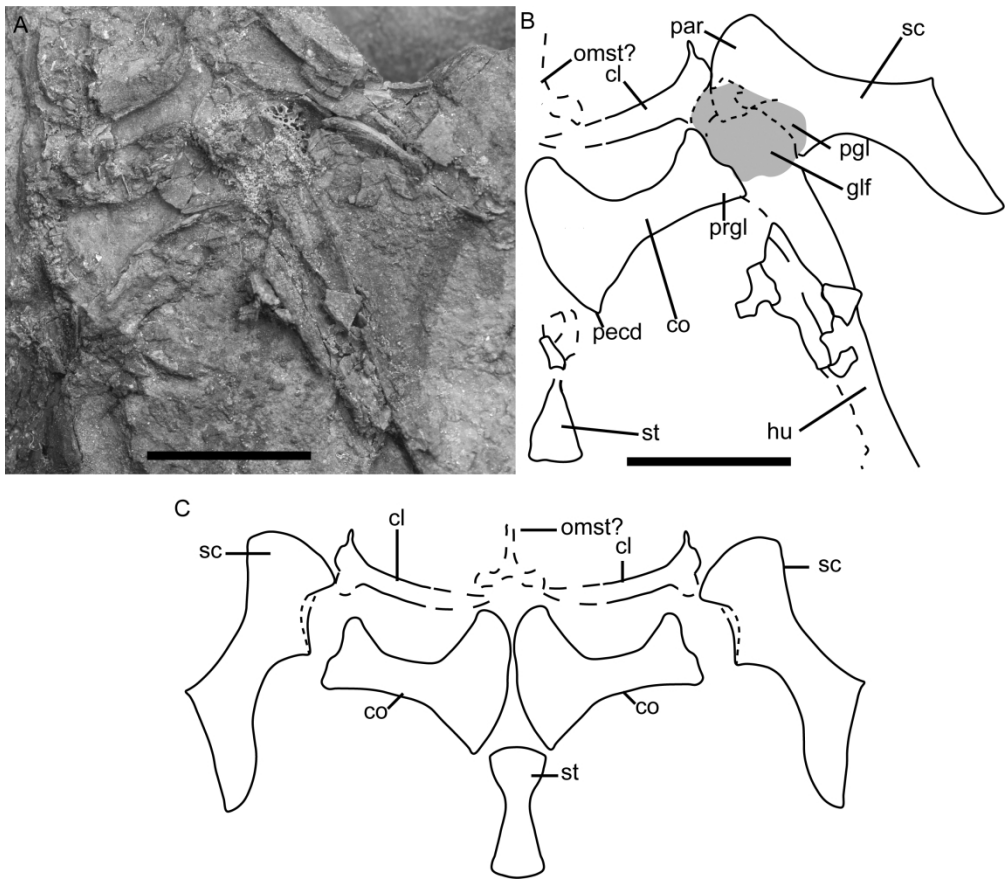

Pectoral elements of IGR 144547. **A**, close-up on the right pectoral region of IGR 144547 on M1, **B**, interpretative drawing of the same region and **C**, reconstruction of the pectoral girdle in ventral view. Light gray area represents the glenoid region. . **Abbreviations**: **cl**, clavicle; **co**, coracoid; **glf**, glenoid fossa?; **hu**, humerus; **omst?**, putative omosternum; **par**, pars acromialis; **pecd**, processus epicoracoidalis; **pgl**, pars glenoidalis; **prgl**, processus glenoidalis; **sc**, scapula; **st**, sternum. Scale bar is 5 mm.

122x106mm (600 x 600 DPI)

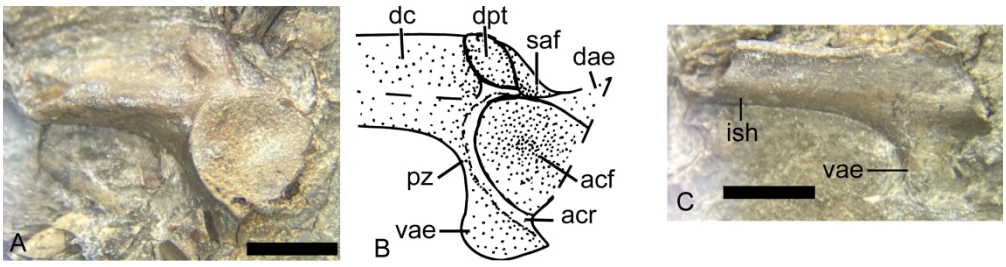

Ilium of IGR144547. **A**, acetabular region of the left ilium exposed in lateral view on M2, **B**, proposed reconstruction of the acetabular region of the left ilium in lateral view and **C**, right ilium in exposed in medial view on M2. Scale bars represent 2 mm. **Abbreviations**: **acf**, acetabular fossa; **acr**, acetabular rim; **dae**, dorsal acetabular expansion; **dc**, dorsal crest; **dpm**, dorsal prominence; **dpt**, dorsal protuberance; **ish**, ilial shaft; **pz**, preacetabular zone; **saf**, supraacetabular fossa; **vae**, ventral acetabular expansion.

181x46mm (600 x 600 DPI)

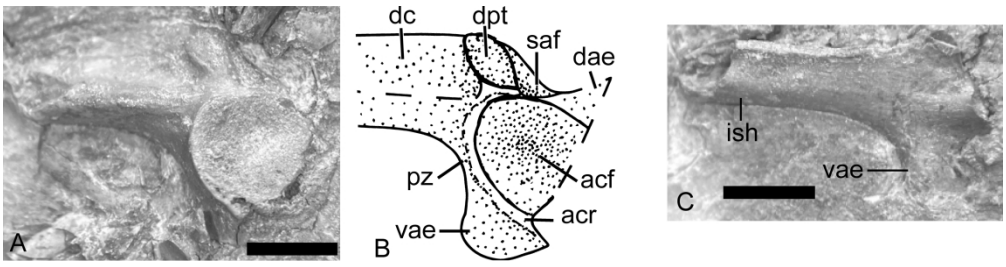

Ilium of IGR144547. **A**, acetabular region of the left ilium exposed in lateral view on M2, **B**, proposed reconstruction of the acetabular region of the left ilium in lateral view and **C**, right ilium in exposed in medial view on M2. Scale bars represent 2 mm. **Abbreviations**: **acf**, acetabular fossa; **acr**, acetabular rim; **dae**, dorsal acetabular expansion; **dc**, dorsal crest; **dpm**, dorsal prominence; **dpt**, dorsal protuberance; **ish**, ilial shaft; **pz**, preacetabular zone; **saf**, supraacetabular fossa; **vae**, ventral acetabular expansion.

181x46mm (600 x 600 DPI)

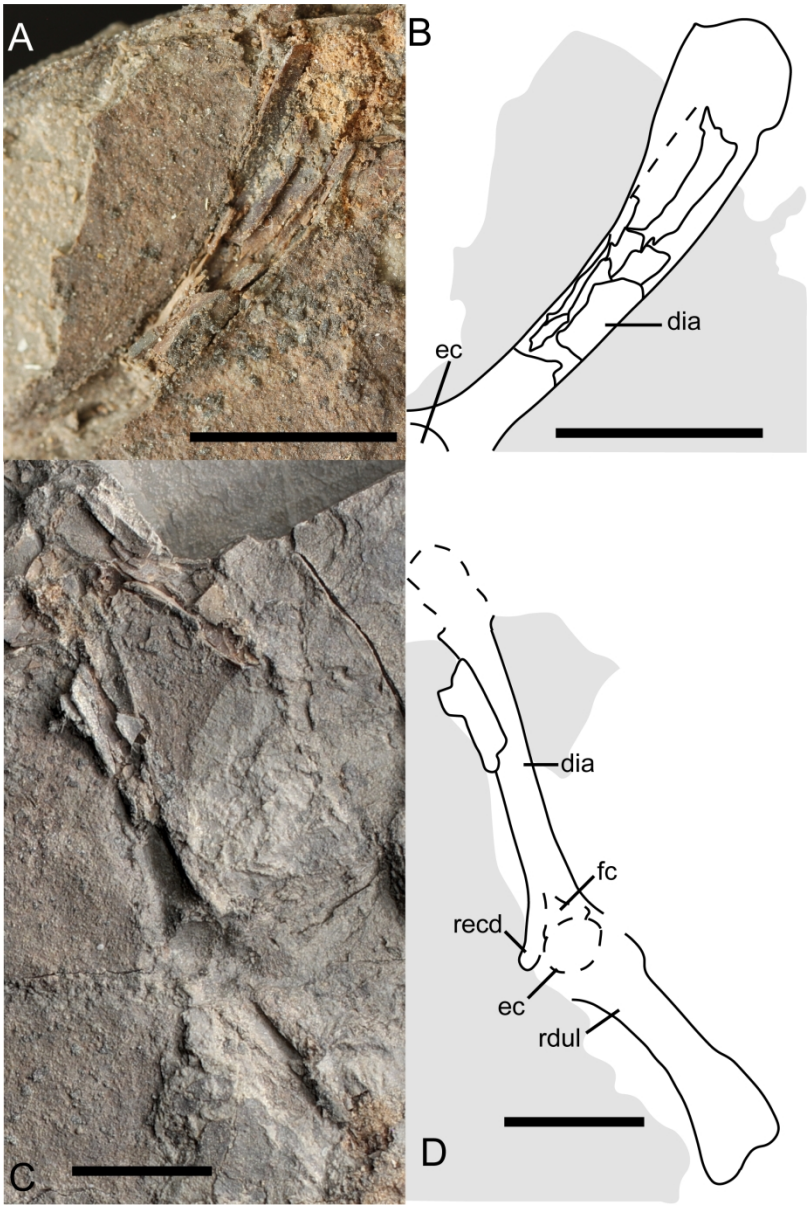

Forelimbs of IG144547. **A**, left humerus on M1, **B**, interpretative drawing of the same humerus, **C**, right forelimb on M1 and **D**, interpretive drawing of the same forelimb. Light gray area represents skin impressions, scale bars represent 5 mm. **Abbreviations**: **ec**, eminetia capitata; **dia**, diaphysis; **fc**, fossa cubitalis; **hb**, humeral ball; **raf**, radiale articular facet ; **recd**, epicondylus radialis.

88x132mm (600 x 600 DPI)

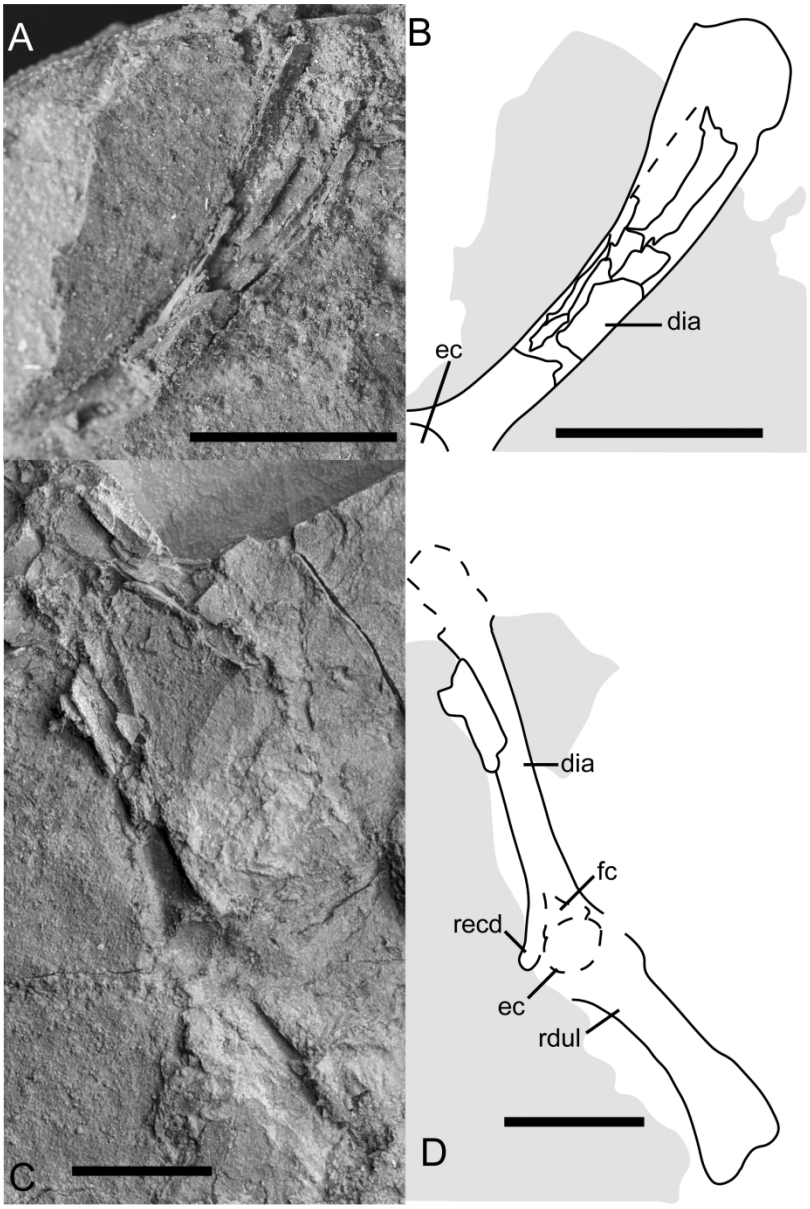

Forelimbs of IG144547. **A**, left humerus on M1, **B**, interpretative drawing of the same humerus, **C**, right forelimb on M1 and **D**, interpretive drawing of the same forelimb. Light gray area represents skin impressions, scale bars represent 5 mm. **Abbreviations**: **ec**, eminetia capitata; **dia**, diaphysis; **fc**, fossa cubitalis; **hb**, humeral ball; **raf**, radiale articular facet ; **recd**, epicondylus radialis.

88x132mm (600 x 600 DPI)

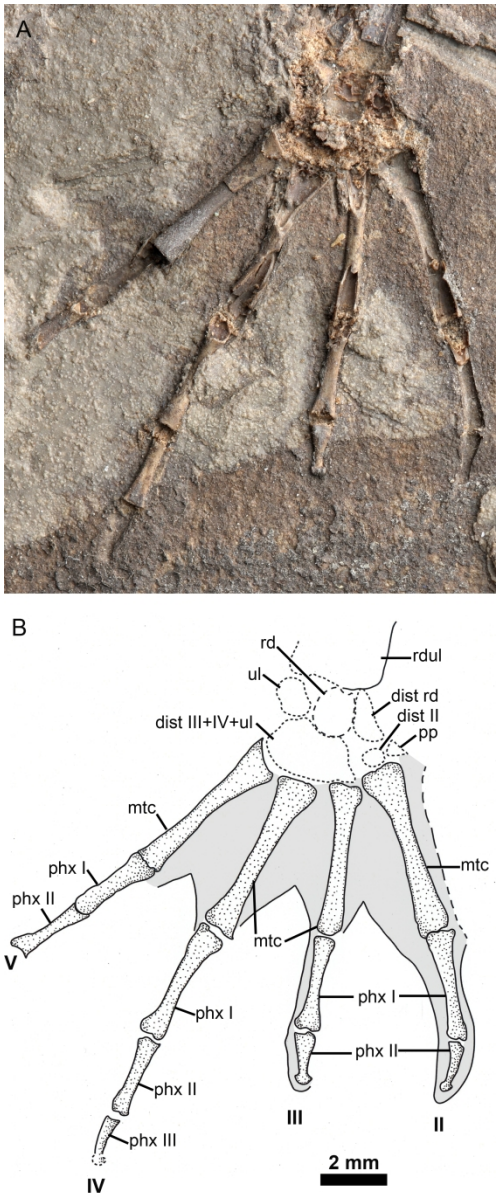

Hand of IGR 144547. **A**, left hand on M1 and **B**, interpretative drawing of the same hand. Light gray areas represent skin impressions of the digits, scale bar represents 2 mm. **Abbreviations**: **dis rd**, distal radiale; **dist ul**, distal ulnare; **dist II**, distal carpale II; **dist III**, distal carpale III; **dist IV**, distal carpale IV; **mtc**, metacarpal; **phx I**, **II**, **III**, phalanx I, II, III; **pp**, prepollex; **rd**, radiale; **rdul**, radioulna; **ul**, ulnare.

88x216mm (600 x 600 DPI)

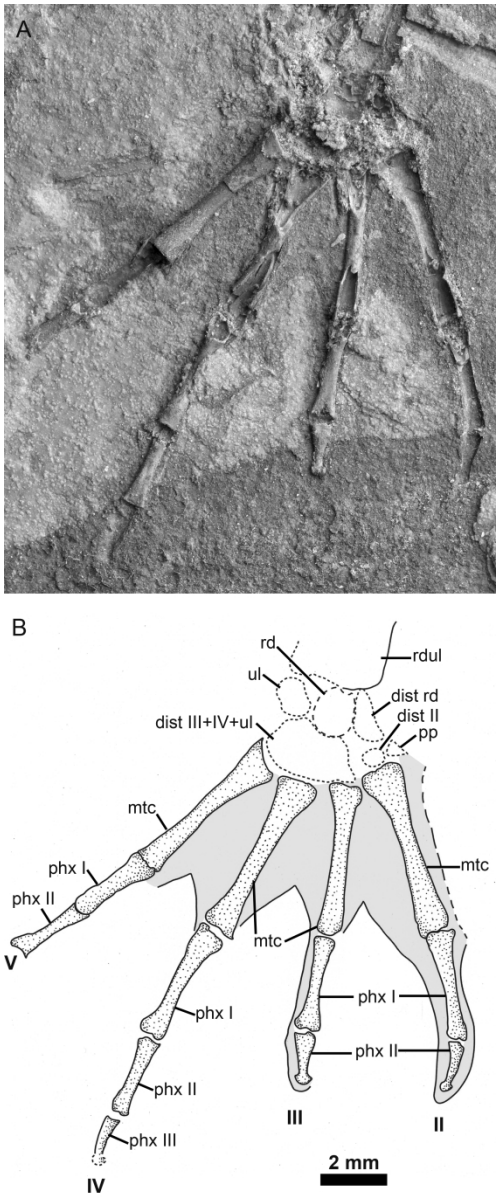

Hand of IGR 144547. **A**, left hand on M1 and **B**, interpretative drawing of the same hand. Light gray areas represent skin impressions of the digits, scale bar represents 2 mm. **Abbreviations**: **dis rd**, distal radiale; **dist ul**, distal ulnare; **dist II**, distal carpale II; **dist III**, distal carpale III; **dist IV**, distal carpale IV; **mtc**, metacarpal; **phx I**, **II**, **III**, phalanx I, II, III; **pp**, prepollex;**rd**, radiale; **rdul**, radioulna; **ul**, ulnare.

88x216mm (600 x 600 DPI)

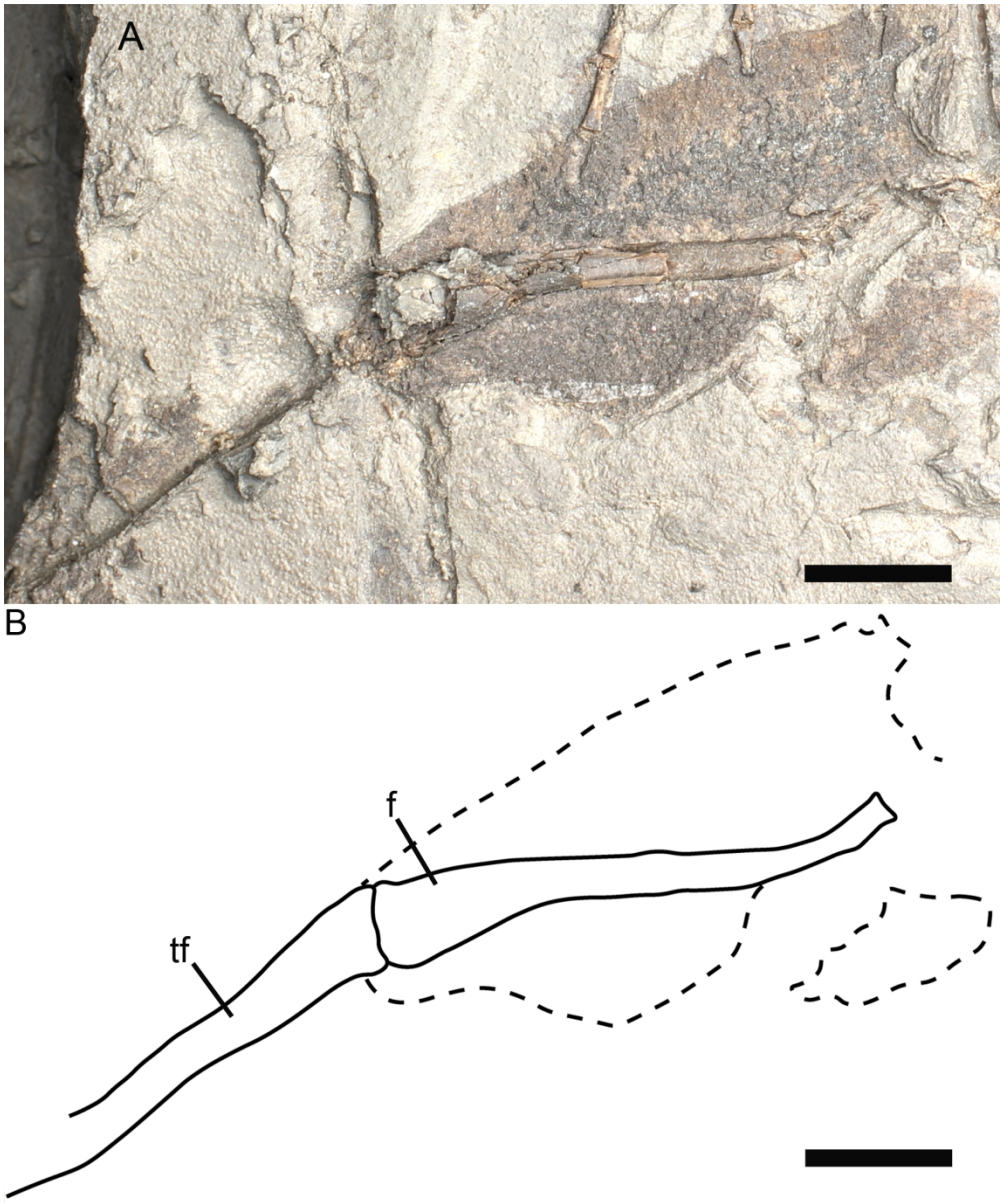

Hindlimb of IGR 144547. **A**, right hindlimb on M1 and **B**, interpretative drawing of the same hindlimb. **Abbreviations**: **f**, femur; **tf**, tibiofibula. Dotted lines delimit skin impressions, scale bar is 5 mm.

88x107mm (600 x 600 DPI)

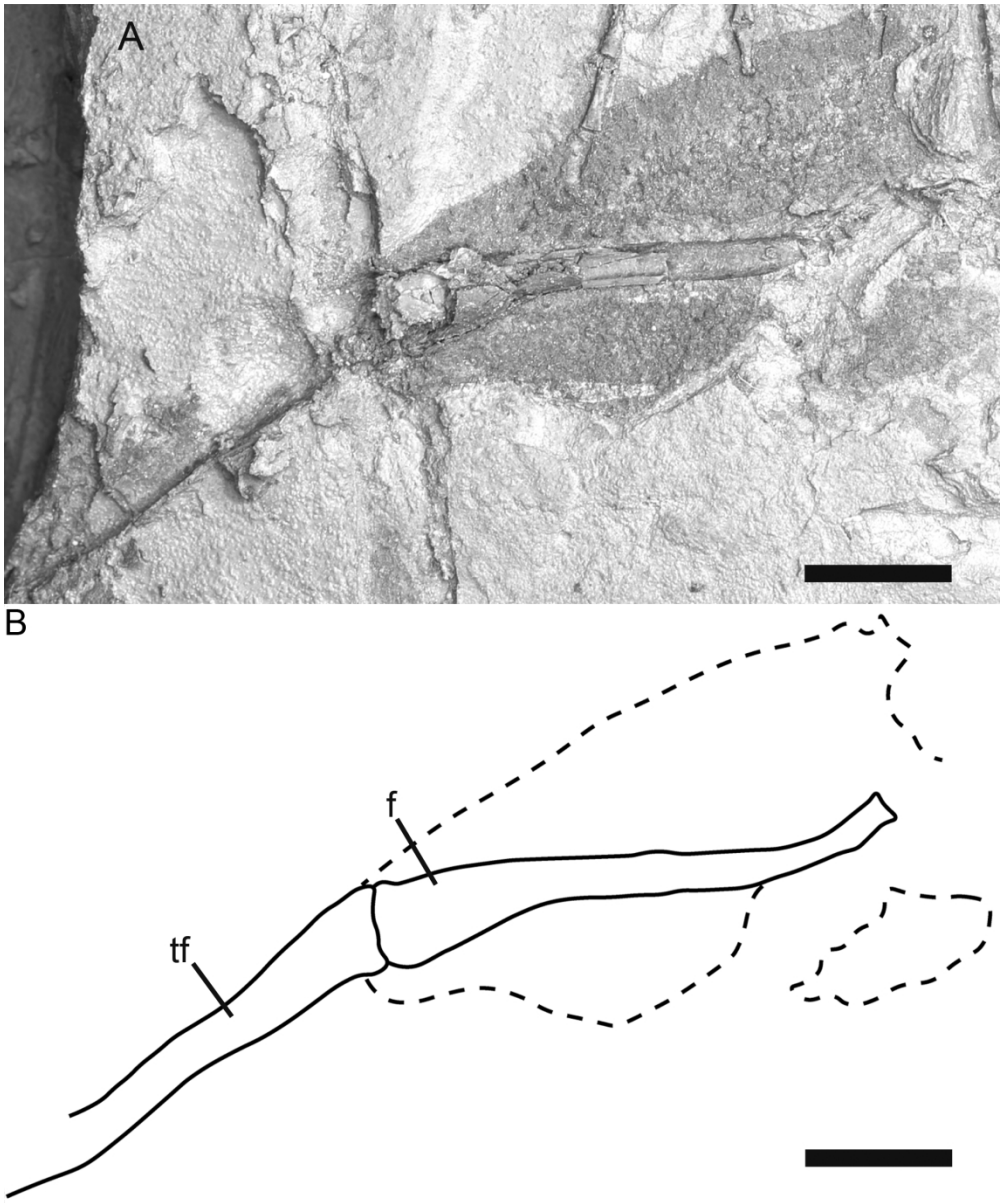

Hindlimb of IGR 144547. **A**, right hindlimb on M1 and **B**, interpretative drawing of the same hindlimb. **Abbreviations**: **f**, femur; **tf**, tibiofibula. Dotted lines delimit skin impressions, scale bar is 5 mm.

88x107mm (600 x 600 DPI)

Journal of Vertebrate Paleontology

Supplementary Data 1

The oldest articulated ranid from Europe: A *Pelophylax* specimen from the earliest Oligocene of Chartres-de -Bretagne (NW France)

ALFRED LEMIERRE,*[.1] DAMIEN GENDRY,[2] MARIE-MARGAUX POIRIER,[2] VALENTIN GILLET,[2] and ROMAIN VULLO[2]

[1]Centre de Recherche en Paléontologie (CR2P) Paris, UMR 7207 CNRS-Muséum National d'Histoire Naturelle-Sorbonne Université, CP38, 8 rue Buffon, 75005 Paris, France, alfred.lemierre@outlook.com;

[2]Université Rennes, Géosciences, UMR CNRS 6118, Campus de Beaulieu, 263 avenue du Général Leclerc, 35042 Rennes, France, mariemargaux.poirier@orange.fr, valentin.gillet.37@gmail.com, romain.vullo@univ-rennes.fr, damien.gendry@univ-rennes.fr

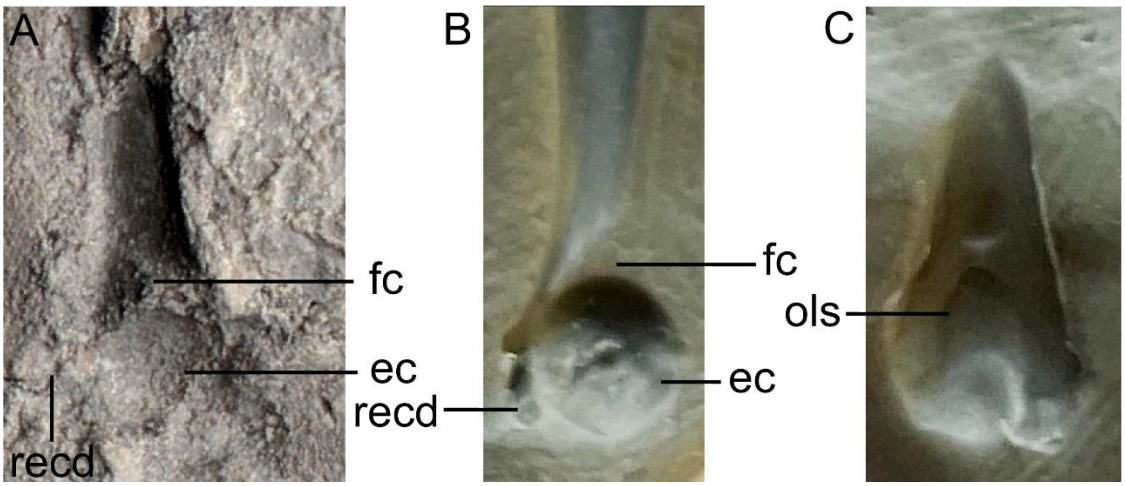

FIGURE S1. Comparison between the imprint of the humerus of IGR 144547 and the humerus of *Pelophylax* kl. *esculentus*. **A**, imprint of a humerus of IGR 144547 on M1, **B**, imprint of a humerus of *P.* kl. *esculentus* in ventral view and **C**, imprint of the same humerus in dorsal view. Abbreviations: **ec**, eminetia capitate; **fc**, fossa cubitalis; **ols**, oleocranon scar; **recd**, epicondylus radialis.